

DESY 98–195
KA–TP–20–1998
hep-ph/9812298v2
July 1999

Top Dipole Form Factors and Loop–induced CP violation in Supersymmetry

W. Hollik^{a,b}, J.I. Illana^c, S. Rigolin^d
C. Schappacher^a, D. Stöckinger^a

^a *Institut für Theoretische Physik, Universität Karlsruhe,
D–76128 Karlsruhe, Germany*

^b *Theoretical Physics Division, CERN,
CH–1211 Geneva 23, Switzerland*

^c *Deutsches Elektronen–Synchrotron DESY,
D–15738 Zeuthen, Germany*

^d *Departamento de Física Teórica, Universidad Autónoma de Madrid,
Cantoblanco, E–28049 Madrid, Spain*

Abstract

The one–loop Minimal Supersymmetric Standard Model (MSSM) contributions to the weak and electromagnetic dipole form factors of the top quark are presented. Far from the Z peak, they are not sufficient to account for all the new physics effects. In the context of the calculation of the process $e^+e^- \rightarrow t\bar{t}$ to one loop in the MSSM, we compare the impact on the phenomenology of the CP–violating dipole form factors of the top quark with the contribution from CP–violating box graphs. Some exemplificative observables are analyzed and the relevance of both the contributions is pointed out. The one–loop expressions for the electromagnetic and weak dipole form factors in a general renormalizable theory and the SM and MSSM couplings and conventions are also given.

1 Introduction

The investigation of the electric and magnetic dipole moments of fermions provides deep insight in particle theory. The measurement of the intrinsic *magnetic dipole moment* (MDM) of the electron proved the correctness of the hypothesis of half-integer-spin particles [1] and is one of the most spectacular achievements of quantum field theory predictions. More precise studies of electron and muon showed afterwards the presence of *anomalous* contributions to the MDM (AMDM). Their predictions constitute one of the most spectacular achievements of Quantum Field Theory and imply very accurate tests of the quantum structure of the Standard Model (SM). The measurements of the $(g_e - 2)$ and $(g_\mu - 2)$ available [2] are in perfect agreement with the SM predictions to several orders in the perturbative expansion of the theory (cf. [3] and references therein). Furthermore, with the expected precision at the E821 Brookhaven experiment [4] it will be possible to improve the previous measurement of $(g_\mu - 2)$ by a factor 20. Therefore the MDMs can be used, together with the precision tests at the Z resonance from LEP and SLC and the new results of LEP2 and TEVATRON, to set bounds on possible new physics effects beyond the SM [5].

The importance of the analysis of the *electric dipole moment* (EDM) of elementary and composite particles is intimately related to the CP violating character of the theory. In the electroweak SM there is only one possible source of CP violation, the δ_{CKM} phase of the Cabibbo–Kobayashi–Maskawa (CKM) mixing matrix for quarks [6]. Currently the only place where CP violation has been measured, the neutral K system, fixes the value of this phase but does not constitute itself a test for the origin of CP violation [7]. On the other hand, if the baryon asymmetry of the universe has been dynamically generated, CP must be violated. The SM cannot account for the size of the observed asymmetry [8]. In extended models (beyond the SM) many other possible explanations of CP violation can be given. In particular, in supersymmetric (SUSY) models [9, 10] CP violation can appear assuming complex soft–SUSY–breaking terms. Two physical phases remain in the GUT constrained MSSM [10, 11, 12], enough to provide the correct size of baryon asymmetry in some range of parameters [13]. But the most significant effect of the CP violating phases in the phenomenology is their contribution to the EDMs [14]. Unlike the SM, where the contribution to the EDM of fermions arises beyond two loops [15], the MSSM can give a contribution already at the one-loop level [9].

The measurements of the neutron, electron and muon EDMs [16, 17] constrain the phases and the supersymmetric spectrum in a way that *may* demand fine tuning (supersymmetric CP problem): either the SUSY particles very heavy (several TeV [18]) or the phases are of $\mathcal{O}(10^{-2})$ [9]. Very large soft–SUSY–breaking masses are unappealing as it seems natural to demand the SUSY spectrum to be at the electroweak scale.¹ On the other side, the experimental constraints can be met taking general universal soft–SUSY–breaking terms and

¹Moreover if the SUSY spectrum is in the TeV region this could also give rise to relic densities unacceptably large.

vanishing SUSY CP phases. In this case the CP violation is originated via the usual SM CKM mechanism and the supersymmetric spectrum affects the observables only through radiative contributions. In this scenario it is difficult to construct models in which the SUSY phases naturally vanish [19] and at the same time provide some other non-standard mechanism for explaining electroweak baryogenesis. There exist also ways of naturally obtaining small non-zero SUSY CP phases which leave sufficient CP violation for baryogenesis [12]. But, in general, they do not lead to observable differences from the SM. In models with potentially observable predictions one has to relax the assumption of soft-term universality. Several attempts have been made, following this direction, to use CP violation from top-squark mixing: a complex parameter A_t would yield large CP violating effects in collider processes involving top quarks [20, 56].² Besides, due to renormalization-group relations, the phase of A_t is constrained by the EDM of the neutron [22]. One can satisfy the experimental constraints due to cancellation among the different components of the neutron EDM (constituent quarks and gluons), the SUSY phases can still be kept of $\mathcal{O}(1)$ and the SUSY spectrum at the electroweak scale satisfying the experimental bounds [23]. In [24, 25] it is shown that large CP violating phases in the MSSM are compatible with the bounds on the electron and neutron EDMs as well as with the cosmological relic densities. In view of all these arguments we keep our analysis completely general and consider the SUSY CP-phases as free parameters.

Some attention has also been paid to the study of possible CP violating effects in the context of R-parity violating models [26]. In this class of models new interactions appear providing extra sources of CP violation (still preventing fast proton decay). They can explain the CP violation in the K system (with no need of the CKM phase) without introducing anomalous Flavor Changing Neutral Current (FCNC) contributions [27]. In the following we restrict our discussion to the simpler case of models with conserved R-parity.

In addition a certain amount of investigation has been devoted to the analysis of *weak dipole moments* (WDM). The WDMs are defined, in analogy to the usual DMs, taking the corresponding on-shell chirality-flipping form factors of the Zff effective vertex. The SM one-loop contribution to the *anomalous weak magnetic dipole moment* (AWMDM) has been calculated for the τ lepton and the b quark in [28, 29]. The CP-violating *weak electric dipole moment* (WEDM) is in the SM a tiny three-loop effect. The WDMs are gauge invariant and can directly connected to physical observables. While for the τ case, using appropriate observables [28, 30, 31], an experimental analysis is feasible, for the b case the situation is complicated by hadronization effects [32]. The SM predictions are far below the sensitivity reachable at LEP [28] but non-standard interactions can enhance these expectations (2HDM [33], MSSM [34]) especially for the (CP-violating) WEDMs (2HDM [35], leptoquark models [36], MSSM [37]). The experimental detection of non-zero AWMDM or WEDM of heavy fermions, at the current sensitivity, would be a clear evidence of new physics beyond the SM.

²Large non-SM CP violating top-quark couplings could be probed at high energy colliders like the NLC [21].

In the perspective of the next generation of linear e^+e^- colliders, we extend the previous analyses on the WDMs to consider the t quark *dipole form factors* (DFF) and, in particular, the CP-violating ones. In [38] an independent analysis of the t quark EDFF and WEDFF can be found. Since the t quark is very heavy one expects this fermion to be the best candidate to have larger DFFs. Beyond the Z peak ($s > 4m_t^2$) other effects are expected to give contributions to the physical observables. In fact the DFFs in a general model are not guaranteed to be gauge independent. An exception is the one-loop MSSM contribution to the CP-violating *electromagnetic* and *weak* DFFs (EDFF and WEDFF) which do not involve any gauge boson in internal lines. Anyway, although this contribution is indeed gauge invariant any CP-odd observable will be sensitive to not only the DFFs but to the complete set of one-loop CP-violating diagrams involved. In this work we present the full calculation of the expectation value of a set of these observables in the context of the MSSM and compare the size of the different contributions.

The paper is organized as follows. In Section 2 we present the general effective vertex describing the interaction of on-shell fermions with a neutral vector boson. The definitions and the generic expressions of the DFFs for all the contributing topologies at the one-loop level are given. In Section 3 we briefly discuss the cancellation of the dipoles in the supersymmetric limit. The numerical results for the t quark EDFFs and WEDFFs at $\sqrt{s} = 500$ GeV are presented in Section 4. In Section 5 we evaluate specific CP-odd observables for the t quark pair production in e^+e^- colliders to one loop in the MSSM and compare the influence of the t EDFF and WEDFF with that of the CP-violating box diagrams. Our conclusions are presented in Section 6. In the Appendices one can find the definition of the one-loop 3-point tensor integrals employed in the expressions for the dipoles as well as the SM and MSSM couplings and conventions that have been used.

2 The dipole form factors

2.1 The Vff effective vertex

The most general effective Lagrangian describing the interaction of a neutral vector boson V with two fermions can be written, using at most dimension five operators, as a function of ten independent terms:

$$\begin{aligned}
\mathcal{L}_{Vff} = & V^\mu(x)\bar{\Psi}(x)\left[\gamma_\mu(g_V - g_A\gamma_5) + i\overleftrightarrow{\partial}_\mu(g_M + ig_E\gamma_5)\right. \\
& \left.+ i\overleftrightarrow{\partial}^\nu\sigma_{\mu\nu}(g_{TS} + ig_{TP}\gamma_5)\right]\Psi(x) \\
& + (i\partial^\mu V^\nu(x))\bar{\Psi}(x)\left[g_{\mu\nu}(ig_S + g_P\gamma_5) + \sigma_{\mu\nu}(ig_{TM} + g_{TE}\gamma_5)\right]\Psi(x). \quad (1)
\end{aligned}$$

Table 1: C , P , T properties of the operators in the effective Lagrangian of Eq. (1). Their chirality flipping behavior is also displayed.

Operator	Coefficient	P	CP	T	Chirality Flip
$V^\mu \bar{\Psi} \gamma_\mu \Psi$	g_V	+	+	+	NO
$V^\mu \bar{\Psi} \gamma_\mu \gamma_5 \Psi$	g_A	-	+	+	NO
$V^\mu \bar{\Psi} i \overleftrightarrow{\partial}_\mu \Psi$	g_M	+	+	+	YES
$V^\mu \bar{\Psi} \overleftrightarrow{\partial}_\mu \gamma_5 \Psi$	g_E	-	-	-	YES
$V^\mu \bar{\Psi} i \overleftrightarrow{\partial}^\nu \sigma_{\mu\nu} \Psi$	g_{TS}	+	-	-	YES
$V^\mu \bar{\Psi} \overleftrightarrow{\partial}^\nu \sigma_{\mu\nu} \gamma_5 \Psi$	g_{TP}	-	+	+	YES
$(\partial \cdot V) \bar{\Psi} \Psi$	g_S	+	-	-	YES
$(i\partial \cdot V) \bar{\Psi} \gamma_5 \Psi$	g_P	-	+	+	YES
$(\partial^\mu V^\nu) \bar{\Psi} \sigma_{\mu\nu} \Psi$	g_{TM}	+	+	+	YES
$(i\partial^\mu V^\nu) \bar{\Psi} \sigma_{\mu\nu} \gamma_5 \Psi$	g_{TE}	-	-	-	YES

The first two coefficients, i.e. g_V and g_A , are the usual vector and axial–vector couplings. They are connected to chirality conserving dimension four operators. All the other coefficients in Eq. (1) multiply chirality flipping dimension five operators and can receive a contribution only through radiative corrections in a renormalizable theory. The operators associated to g_V , g_A , g_M , g_P , g_{TM} and g_{TP} are even under a CP transformation. The presence of non vanishing g_E , g_S , g_{TE} and g_{TS} yields a contribution to CP–violating observables. In Table 1 we summarize the C, P, T and chirality properties of each operator introduced in the effective Lagrangian.

By Fourier transform of Eq. (1) one obtains the most general Lorentz structure for the vertex Vff in the momentum space:

$$\Gamma_\mu^{Vff} = i \left[\gamma_\mu (f_V - f_A \gamma_5) + (q - \bar{q})_\mu (f_M + i f_E \gamma_5) + p_\mu (i f_S + f_P \gamma_5) \right. \\ \left. + (q - \bar{q})^\nu \sigma_{\mu\nu} (f_{TS} + i f_{TP} \gamma_5) + p^\nu \sigma_{\mu\nu} (i f_{TM} + f_{TE} \gamma_5) \right], \quad (2)$$

where q and \bar{q} are the outgoing momenta of the fermions and $p = (q + \bar{q})$ is the total incoming momentum of the neutral boson V . The form factors f_i are functions of the kinematical invariants. Actually they are more general than the coefficients g_i . In fact any operator of dimension higher than five added to the Lagrangian of Eq. (1) is related to a new coefficient g_i . But every new coefficient can contribute only to the ten independent form factors f_i introduced in Eq. (2). The parameters g_i and the form factors f_i can be complex in general.

Their real parts account for dispersive effects (CPT-even) whereas their imaginary parts are related to absorptive contributions.

It is possible to lower the number of independent form factors in Eq. (2) by imposing on-shell conditions on the fermionic and/or bosonic fields. For instance, in the case of on-shell fermions, making use of the Gordon identities:

$$\begin{aligned}
2m_f \bar{u} \gamma^\mu v &= \left\{ \bar{u} (q - \bar{q})^\mu v + \bar{u} i (q + \bar{q})_\nu \sigma^{\mu\nu} v \right\}, \\
2m_f \bar{u} \gamma^\mu \gamma_5 v &= \left\{ \bar{u} (q + \bar{q})^\mu \gamma_5 v + \bar{u} i (q - \bar{q})_\nu \sigma^{\mu\nu} \gamma_5 v \right\}, \\
0 &= \left\{ \bar{u} (q + \bar{q})^\mu v + \bar{u} i (q - \bar{q})_\nu \sigma^{\mu\nu} v \right\}, \\
0 &= \left\{ \bar{u} (q - \bar{q})^\mu \gamma_5 v + \bar{u} i (q + \bar{q})_\nu \sigma^{\mu\nu} \gamma_5 v \right\}, \tag{3}
\end{aligned}$$

one can eliminate f_{TM} , f_{TE} , f_{TS} and f_{TP} from the effective Lagrangian. The number of relevant form factors can be further reduced taking also the boson V on its mass shell. In this case the condition $p_\mu e^\mu = 0$ automatically cancels all the contributions coming from f_{S} and f_{P} . The same situation occurs for off-shell vector boson V when, in the process $e^+e^- \rightarrow V^* \rightarrow f\bar{f}$, the electron mass is neglected. Therefore f_{S} and f_{P} will be ignored in the following. With all these assumptions the Vff effective vertex for on-shell fermions is conventionally written as:

$$\Gamma_\mu^{Vff}(s) = ie \left\{ \gamma_\mu \left[V_f^V(s) - A_f^V(s) \gamma_5 \right] + \sigma_{\mu\nu} (q + \bar{q})^\nu \left[i \frac{a_f^V(s)}{2m_f} - \frac{d_f^V(s)}{e} \gamma_5 \right] \right\}, \tag{4}$$

where e and m_f are respectively the electric unit charge and the mass of the external fermion. The form factors in Eq. (4) depend only on s . As mentioned above $V_f^V(s)$ and $A_f^V(s)$ parameterize the vector and axial-vector current. They are connected to the chirality conserving CP-even sector. The form factors $a_f^V(s)$ and $d_f^V(s)$ are known respectively as anomalous magnetic dipole form factor (AMDFF) and electric dipole form factor (EDFF). They are both connected to chirality flipping operators. In a renormalizable theory they can receive contributions exclusively by quantum corrections. The EDFFs contribute to the CP-odd sector and constitute a source of CP-violation.

The *dipole moments* (DM) are defined taking the corresponding vector bosons on shell, $s = M_V^2$. For $V = \gamma$ one gets the usual definitions of the photon *anomalous magnetic dipole moment* (AMDM) and *electric dipole moment* (EDM). The definitions of electric charge, magnetic and electric dipole moments [39] consistent with our convention for the covariant derivative (62) are respectively:

$$\text{charge} \equiv -e V_f^\gamma(0) = e Q_f, \tag{5}$$

$$\text{MDM} \equiv \frac{e}{2m_f} (V_f^\gamma(0) + a_f^\gamma(0)), \tag{6}$$

$$\text{EDM} \equiv d_f^\gamma(0). \tag{7}$$

Thus the AMDM of a fermion is $a_f^\gamma(0) = -Q_f(g_f - 2)/2$ with g_f being the gyromagnetic ratio. The axial-vector coupling A_f^γ vanishes. For $V = Z$, the quantities $a_f^w \equiv a_f^Z(M_Z^2)$

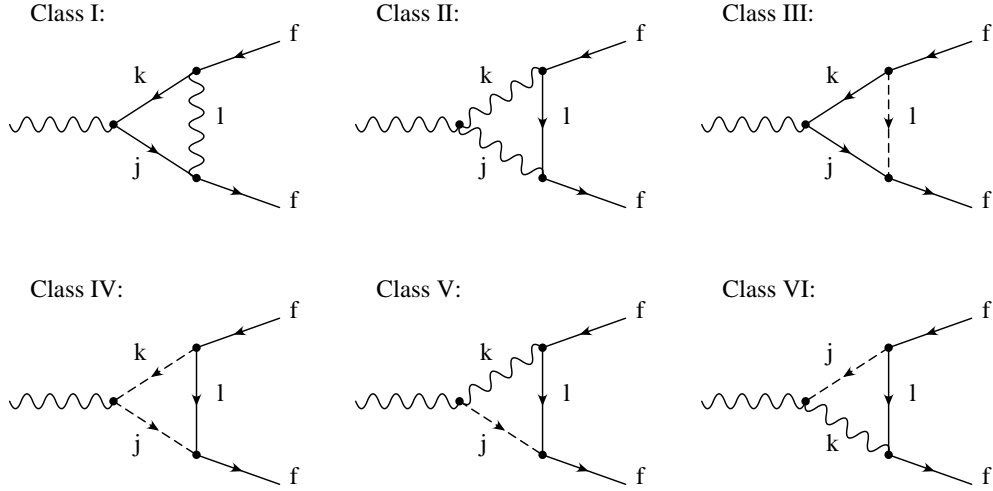


Figure 1: *The one-loop Vff diagrams with general couplings.*

and $d_f^w \equiv d_f^Z(M_Z^2)$ define the *anomalous weak-magnetic dipole moment* (AWMDM) and the *weak-electric dipole moment* (WEDM).³

2.2 One-loop generic expressions of the dipole form factors

All the possible one-loop contributions to the $a_f^V(s)$ and $d_f^V(s)$ form factors can be classified in terms of the six classes of triangle diagrams depicted in Fig. 1. The vertices involved are labeled by generic couplings for vector bosons $V_\mu^{(k)} = A_\mu, Z_\mu, W_\mu, W_\mu^\dagger$, fermions Ψ_k and scalar bosons Φ_k , according to the following interaction Lagrangian:

$$\begin{aligned} \mathcal{L} = & ieJ(W_{\mu\nu}^\dagger W^\mu V^\nu - W^{\mu\nu} W_\mu^\dagger V_\nu + V^{\mu\nu} W_\mu^\dagger W_\nu) + ieG_{jk} V^\mu \Phi_j^\dagger \overleftrightarrow{\partial}_\mu \Phi_k \\ & + \left\{ e\bar{\Psi}_f(S_{jk} - P_{jk}\gamma_5)\Psi_k\Phi_j + eK_{jk}V^\mu V_\mu^{(k)}\Phi_j + \text{h.c.} \right\} \\ & + eV_\mu^{(k)}\bar{\Psi}_j\gamma^\mu(V_{jl}^{(k)} - A_{jl}^{(k)}\gamma_5)\Psi_l. \end{aligned} \quad (8)$$

Every class of diagrams is calculated analytically and expressed in terms of the couplings introduced in (8) and the one-loop 3-point integrals \bar{C}_i (see App. A). The result is given in the 't Hooft-Feynman gauge.

- [Class I]: vector-boson exchange:

$$\frac{a_f^V(s)}{2m_f}(\text{I}) = \frac{\alpha}{4\pi} \left\{ 4m_f \sum_{jkl} \text{Re} \left[V_{jk}^{(V)} (V_{fj}^{(l)} V_{fk}^{(l)*} + A_{fj}^{(l)} A_{fk}^{(l)*}) \right] \right.$$

³Massless and neutral fermions may have magnetic moments. The usual parameterization in (4) must be generalized by the replacement $e a_f^V(s)/2m_f \rightarrow \mu^V(s)$. The dipole moments of neutrinos are then given by $\mu^V(M_V^2)$.

$$\begin{aligned}
& + A_{jk}^{(V)} (V_{fj}^{(l)} A_{fk}^{(l)*} + A_{fj}^{(l)} V_{fk}^{(l)*}) \left[2C_2^+ - 3C_1^+ + C_0 \right]_{kjl} \\
& + 4 \sum_{jkl} m_k \text{Re} \left[V_{jk}^{(V)} (V_{fj}^{(l)} V_{fk}^{(l)*} - A_{fj}^{(l)} A_{fk}^{(l)*}) \right. \\
& \quad \left. - A_{jk}^{(V)} (V_{fj}^{(l)} A_{fk}^{(l)*} - A_{fj}^{(l)} V_{fk}^{(l)*}) \right] \left[2C_1^+ - C_0 \right]_{kjl} \} \quad (9)
\end{aligned}$$

$$\begin{aligned}
\frac{d_f^V(s)}{e}(\text{I}) &= \frac{\alpha}{4\pi} \left\{ 4m_f \sum_{jkl} \text{Im} \left[V_{jk}^{(V)} (V_{fj}^{(l)} A_{fk}^{(l)*} + A_{fj}^{(l)} V_{fk}^{(l)*}) \right. \right. \\
& \quad \left. \left. + A_{jk}^{(V)} (V_{fj}^{(l)} V_{fk}^{(l)*} + A_{fj}^{(l)} A_{fk}^{(l)*}) \right] \left[2C_2^{+-} - C_1^- \right]_{kjl} \right. \\
& \quad \left. - 4 \sum_{jkl} m_k \text{Im} \left[V_{jk}^{(V)} (V_{fj}^{(l)} A_{fk}^{(l)*} - A_{fj}^{(l)} V_{fk}^{(l)*}) \right. \right. \\
& \quad \left. \left. - A_{jk}^{(V)} (V_{fj}^{(l)} V_{fk}^{(l)*} - A_{fj}^{(l)} A_{fk}^{(l)*}) \right] \left[2C_1^+ - C_0 \right]_{kjl} \right\} \quad (10)
\end{aligned}$$

In the case of gluon exchange one has to substitute α for α_s and $V_{fi}^{(l)}$ for T_l (the SU(3) generators) and take $A_{fj}^{(l)} = 0$. The sum over the index l yields a color factor $C_F = 4/3$. The gluon contribution to the CP-violating form factor $d_f^V(\text{I})$ vanishes in general.

- [Class II]: fermion exchange and two internal vector bosons:

$$\begin{aligned}
\frac{a_f^V(s)}{2m_f}(\text{II}) &= \frac{\alpha}{4\pi} \left\{ 2m_f \sum_{jkl} \text{Re} \left[J(V_{fl}^{(j)} V_{fl}^{(k)*} + A_{fl}^{(j)} A_{fl}^{(k)*}) \right] \left[4C_2^+ + C_1^+ \right]_{kjl} \right. \\
& \quad \left. - 6 \sum_{jkl} m_l \text{Re} \left[J(V_{fl}^{(j)} V_{fl}^{(k)*} - A_{fl}^{(j)} A_{fl}^{(k)*}) \right] \left[C_1^+ \right]_{kjl} \right\} \quad (11)
\end{aligned}$$

$$\begin{aligned}
\frac{d_f^V(s)}{e}(\text{II}) &= -\frac{\alpha}{4\pi} \left\{ 2m_f \sum_{jkl} \text{Im} \left[J(V_{fl}^{(j)} A_{fl}^{(k)*} + A_{fl}^{(j)} V_{fl}^{(k)*}) \right] \left[4C_2^{+-} - C_1^- \right]_{kjl} \right. \\
& \quad \left. + 6 \sum_{jkl} m_l \text{Im} \left[J(V_{fl}^{(j)} A_{fl}^{(k)*} - A_{fl}^{(j)} V_{fl}^{(k)*}) \right] \left[C_1^+ \right]_{kjl} \right\} \quad (12)
\end{aligned}$$

- [Class III]: scalar exchange:

$$\begin{aligned}
\frac{a_f^V(s)}{2m_f}(\text{III}) &= \frac{\alpha}{4\pi} \left\{ 2m_f \sum_{jkl} \text{Re} \left[V_{jk}^{(V)} (S_{lj} S_{lk}^* + P_{lj} P_{lk}^*) \right. \right. \\
& \quad \left. \left. + A_{jk}^{(V)} (S_{lj} P_{lk}^* + P_{lj} S_{lk}^*) \right] \left[2C_2^+ - C_1^+ \right]_{kjl} \right. \\
& \quad \left. - 2 \sum_{jkl} m_k \text{Re} \left[V_{jk}^{(V)} (S_{lj} S_{lk}^* - P_{lj} P_{lk}^*) \right. \right. \\
& \quad \left. \left. - A_{jk}^{(V)} (S_{lj} P_{lk}^* - P_{lj} S_{lk}^*) \right] \left[C_1^+ + C_1^- \right]_{kjl} \right\} \quad (13)
\end{aligned}$$

$$\begin{aligned}
\frac{d_f^V(s)}{e}(\text{III}) &= \frac{\alpha}{4\pi} \left\{ -2m_f \sum_{jkl} \text{Im} \left[V_{jk}^{(V)} (P_{lj} S_{lk}^* + S_{lj} P_{lk}^*) \right. \right. \\
& \quad \left. \left. + A_{jk}^{(V)} (S_{lj} S_{lk}^* + P_{lj} P_{lk}^*) \right] \left[2C_2^{+-} - C_1^- \right]_{kjl} \right. \\
& \quad \left. + 2 \sum_{jkl} m_k \text{Im} \left[V_{jk}^{(V)} (P_{lj} S_{lk}^* - S_{lj} P_{lk}^*) \right. \right.
\end{aligned}$$

$$+A_{jk}^{(V)}(S_{lj}S_{lk}^* - P_{lj}P_{lk}^*)\left[C_1^+ + C_1^-\right]_{kjl}\} \quad (14)$$

- [Class IV]: fermion exchange and two internal scalars:

$$\begin{aligned} \frac{a_f^V(s)}{2m_f}(\text{IV}) &= -\frac{\alpha}{4\pi}\left\{2m_f\sum_{jkl}\text{Re}\left[G_{jk}(S_{jl}S_{kl}^* + P_{jl}P_{kl}^*)\right]\left[2C_2^+ - C_1^+\right]_{kjl}\right. \\ &\quad \left. + \sum_{jkl}m_l\text{Re}\left[G_{jk}(S_{jl}S_{kl}^* - P_{jl}P_{kl}^*)\right]\left[2C_1^+ - C_0\right]_{kjl}\right\} \quad (15) \end{aligned}$$

$$\begin{aligned} \frac{d_f^V(s)}{e}(\text{IV}) &= \frac{\alpha}{4\pi}\left\{2m_f\sum_{jkl}\text{Im}\left[G_{jk}(S_{jl}P_{kl}^* + P_{jl}S_{kl}^*)\right]\left[2C_2^{+-} - C_1^-\right]_{kjl}\right. \\ &\quad \left. - \sum_{jkl}m_l\text{Im}\left[G_{jk}(S_{jl}P_{kl}^* - P_{jl}S_{kl}^*)\right]\left[2C_1^+ - C_0\right]_{kjl}\right\} \quad (16) \end{aligned}$$

- [Class V+VI]: fermion exchange, one vector and one scalar internal boson:

$$\frac{a_f^V(s)}{2m_f}(\text{V + VI}) = \frac{\alpha}{4\pi}2\sum_{jkl}\text{Re}\left[K_{jk}(V_{fl}^{(k)}S_{jl}^* + A_{fl}^{(k)}P_{jl}^*)\right]\left[C_1^+ + C_1^-\right]_{kjl} \quad (17)$$

$$\frac{d_f^V(s)}{e}(\text{V + VI}) = -\frac{\alpha}{4\pi}2\sum_{jkl}\text{Im}\left[K_{jk}(V_{fl}^{(k)}P_{jl}^* + A_{fl}^{(k)}S_{jl}^*)\right]\left[C_1^+ + C_1^-\right]_{kjl} \quad (18)$$

In Eqs. (9–18) the shorthand notation $[\bar{C}]_{kjl}$ stands for the 3–point tensor integrals $\bar{C}(-\bar{q}, q, M_k, M_j, M_l)$. The integrals appearing in the previous Eqs. are UV and IR finite. All the expressions are proportional to some positive power of a fermion mass, either internal or external, consistently with the chirality flipping character of the dipole moments.⁴ For class V and VI diagrams the mass dependence is hidden in the product of the Yukawa couplings S_{ij} (P_{ij}) and the dimensionful parameter K_{ij} . Hence, the heaviest fermions are the most promising candidates to have larger DFFs. Eqs.(9–18) also show that, in general, the DFFs for massless fermions are not vanishing but proportional to masses of fermions running in the loop. The SM cancellation of the massless neutrino DFFs is only due to the absence of right–handed neutrinos. Finally, notice that all the contributions to the EDFFs are proportional to the imaginary part of certain combinations of couplings. A theory with real couplings has manifestly vanishing EDFFs.

3 Cancellation of the dipole moments in the supersymmetric limit

A general Vff interaction is restricted to the form (2) by Lorentz invariance. Since the Lorentz algebra is a subalgebra of supersymmetry, this interaction is even more constrained

⁴This is as expected when applying the mass–insertion method: to induce a flip in the fermion chirality one introduces a mass in either one of the internal fermion lines, picking a mass term from the propagator, or in the external fermion lines, using the equations of motion for the free fermion.

in a theory with unbroken supersymmetry. In [40] supersymmetric sum rules are derived that relate the electric and magnetic multipole moments of any irreducible $N = 1$ supermultiplet. Applied to the Vff interaction between a vector boson coupling to a conserved current and the fermionic component of a chiral multiplet, these sum rules force the gyromagnetic ratio to be $g_f = 2$ and forbid an electric dipole moment:

$$a_f^V = d_f^V = 0. \quad (19)$$

The Lagrangian of the MSSM is supersymmetric when the soft-breaking terms are removed. For non zero value of the μ parameter the Higgs potential has only a trivial minimum. Therefore to keep the particles massive and supersymmetry preserved at the same time the choice $\mu = 0$ is necessary. Then the Higgs potential is positive semi-definite and it has degenerate minima corresponding to $v \equiv v_1 = v_2$ ($\tan\beta = 1$). The value of $M_A = 0$ follows from such a configuration. Finally the value of the common v is fixed by the muon decay constant.

In this supersymmetric limit the above mentioned sum rules are valid and the magnetic and electric dipole form factors have to cancel. To verify our expressions we checked this for the AWMDM of the b quark [37]. Choosing the parameters $A_b = A_t = M_2 = M_3 = 0$, $\mu = 0$, $\tan\beta = 1$ and $M_A = 0$, the SM gauge boson contribution to a_b^w [29] is indeed cancelled by the MSSM correction including the two Higgs doublets: the gluon and gluino contribution cancel among themselves and the neutralinos and charginos cancel the gauge boson and Higgs contributions. A similar check has been performed for the electric and weak-electric dipole form factors of the t quark.

4 SM and MSSM predictions for the top quark dipole form factors

4.1 SM

The electroweak contributions to the magnetic and weak-magnetic dipole form factors for off-shell gauge bosons are gauge dependent. The pinch technique [41] could be used to construct gauge-parameter independent magnetic dipoles in the class of R_ξ gauges [42, 33] but the prescription is not unique [43] and these quantities cannot be observable by themselves. The QCD contributions (gluon exchange) to the t (W)MDFF are gauge independent and comparable in size to the electroweak predictions at $\sqrt{s} = 500$ GeV in the 't Hooft-Feynman gauge [33] due to the large mass of the t quark.

There is no contribution to the electric and weak-electric dipole form factors to one loop in the SM.

4.2 MSSM

The triangle diagrams with SUSY particles are gauge independent by themselves (no gauge or Goldstone bosons involved) but the ones including Higgs scalars and gauge bosons in the loop are not sufficient to keep the gauge invariance in the case of the magnetic dipole form factor. The CP-violating dipole form factors (electric and weak-electric) for which the Higgs sector of the MSSM is irrelevant, on the other hand, can be regarded as gauge independent quantities. These form factors have also been considered in [38] and the numerical results in are in agreement with the ones presented here. Since the MSSM contains a CP-conserving Higgs sector⁵ and the SM provides contributions to the (W)EDMs beyond two loops, the relevant diagrams are the genuine SUSY graphs of classes III and IV.

We investigate the SUSY contributions to the t electric and weak-electric dipole form factors performing a parameter scan for which a fixed value $\sqrt{s} = 500$ GeV has been chosen.⁶ It is important to point out that the region of the supersymmetric parameter space that provides the maximal contributions varies with s due to threshold effects. We scan the mass parameters M_2 and $|\mu|$ in a broad range and the CP-violating phases: φ_μ , $\varphi_{\tilde{t}}$ and $\varphi_{\tilde{b}}$ (see Figs. 2 and 3). The gluino mass ($m_{\tilde{g}} = M_3$) is given by the GUT constraint (75). We adopt a fixed value for the common scalar quark mass $m_{\tilde{q}} = 200$ GeV: this is a plausible intermediate value; larger values decrease the effects. Finally, the moduli of the off-diagonal terms in the \tilde{t} and \tilde{b} mass matrices are also chosen at fixed values $|m_{LR}^t| = |m_{LR}^b| = 200$ GeV, to reduce the number of free parameters. The results are expressed in t magnetons $\mu_t \equiv e/2m_t = 5.64 \times 10^{-17}$ ecm.

The MSSM contributions to the top quark EDFFF and WEDFF are analyzed below.

4.2.1 Neutralinos and \tilde{t} scalar quarks

They provide typically small contributions but quite sensitive to the value of both the phases involved, φ_μ and $\varphi_{\tilde{t}}$ (Fig. 2).

The results are larger for low $\tan\beta$ since the chirality flipping mass terms are dominated by the t quark, yielding a term proportional to $m_t \cot\beta$. A term proportional to the neutralino masses is also present as well as a negligible one proportional to $m_b \tan\beta$. The contributing diagrams belong to the classes III and IV for the Z case and only to class IV for the γ case, as the neutralinos do not couple to photons.

As a reference we take the representative values $M_2 = |\mu| = 200$ GeV and $\varphi_\mu = -\varphi_{\tilde{t}} = \pi/2$. For these inputs the results are

$$d_t^{\tilde{\chi}^0} = (0.080 + 0.081 i) \times 10^{-3} \mu_t, \quad (20)$$

$$d_t^Z[\tilde{\chi}^0] = (-0.324 + 0.223 i) \times 10^{-3} \mu_t. \quad (21)$$

⁵A one-loop non vanishing contribution to the WEDM is possible in a general 2HDM [35].

⁶We use the running coupling constants evaluated at $\sqrt{s} = 500$ GeV, $\alpha_s = 0.092$, $\alpha = 1/126$.

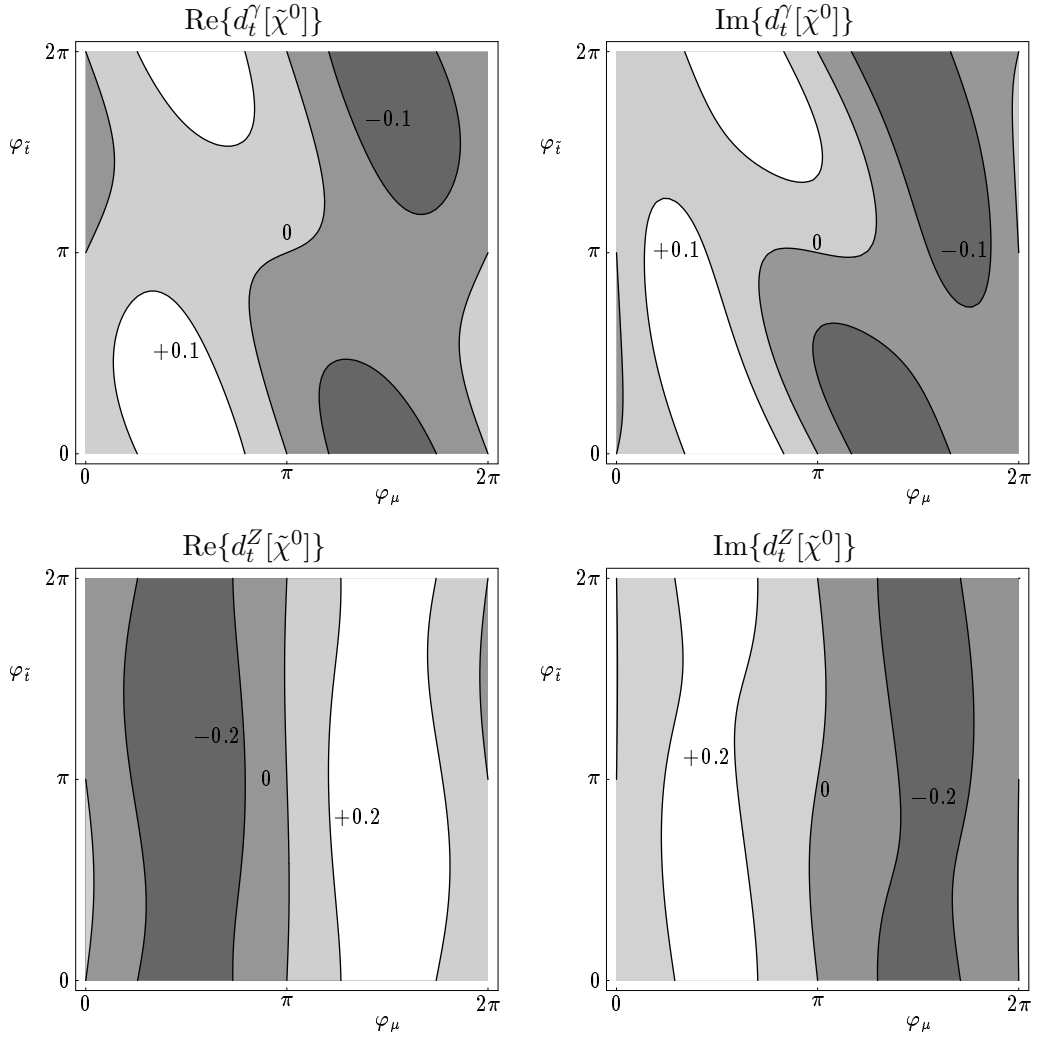


Figure 2: Neutralino contribution to the real and imaginary parts of the t EDF and WEFF [in $10^{-3}\mu_t$ units] in the plane $\varphi_{\tilde{t}} - \varphi_{\mu}$ for $\tan\beta = 1.6$ and the reference values $M_2 = |\mu| = |m_{LR}^t| = 200$ GeV at $\sqrt{s} = 500$ GeV.

4.2.2 Charginos and \tilde{b} scalar quarks

As in the case of the neutralinos, the influence of chargino diagrams is enhanced for low $\tan\beta$.

The results depend very little on $\varphi_{\tilde{b}}$ and mainly on φ_{μ} , the maxima being close to $\varphi_{\mu} = \pm\pi/2$. For increasing $\tan\beta$ the dependence on $\varphi_{\tilde{b}}$ grows, as it comes with a factor proportional to $m_b \tan\beta$.

The chargino contributions are the most important ones. In Fig. 3 the dependence on $\text{Im}(\mu)$ and M_2 is displayed for $\tan\beta = 1.6$. The only relevant CP-violating phase here has been set to the most favorable case, $\varphi_{\mu} = \pi/2$ (the negative values of $\text{Im}(\mu)$ correspond to $\varphi_{\mu} = -\pi/2$). The symmetry with respect to $\text{Im}(\mu) = 0$ in Fig. 3 reflects the (almost) independence of $\varphi_{\tilde{b}}$, here set to $\pi/2$.⁷ The same does not happen for the neutralino contributions for a fixed value of $\varphi_{\tilde{t}} \neq 0, \pi$ in the plane $M_2 - \text{Im}(\mu)$. The plots of Fig. 3 exhibit a tendency to decoupling of the supersymmetric effects for increasing values of the mass parameters [44]. The isolines for a couple of masses of the lightest charginos and neutralinos in the same plane are also given for orientation. The current LEP2 experimental lower limits are $m_{\tilde{\chi}_1^0} \gtrsim 25$ GeV and $m_{\tilde{\chi}_1^{\pm}} \gtrsim 90$ GeV [2].

The chargino contributions for the values $M_2 = |\mu| = 200$ GeV and $\varphi_{\mu} = \pi/2$ are

$$d_t^{\gamma}[\tilde{\chi}^{\pm}] = (0.869 - 1.870 i) \times 10^{-3} \mu_t , \quad (22)$$

$$d_t^Z[\tilde{\chi}^{\pm}] = (0.793 - 2.524 i) \times 10^{-3} \mu_t . \quad (23)$$

4.2.3 Gluinos and \tilde{t} scalar quarks

Their effect is roughly proportional to $|m_{LR}^t| \sin\varphi_{\tilde{t}}$ times a chirality flipping fermion mass, either m_t or M_3 (the gluino mass). It is damped for heavy gluinos circulating in the loop and also for large scalar quark masses due to decoupling. Both terms have opposite sign to $\text{Im}(m_{LR}^t)$ and the one proportional to the gluino mass dominates.

The result for $M_2 = 200$ GeV and $\varphi_{\tilde{t}} = -\pi/2$ is

$$d_t^{\gamma}[\tilde{g}] = (0.457 + 0.170 i) \times 10^{-3} \mu_t , \quad (24)$$

$$d_t^Z[\tilde{g}] = (0.155 + 0.059 i) \times 10^{-3} \mu_t . \quad (25)$$

⁷All the contributions flip sign when the set $(\varphi_{\mu}, \varphi_{\tilde{t}}, \varphi_{\tilde{b}})$ is rotated by π . They vanish accordingly when all the phases are zero. See Fig. 2 for illustration.

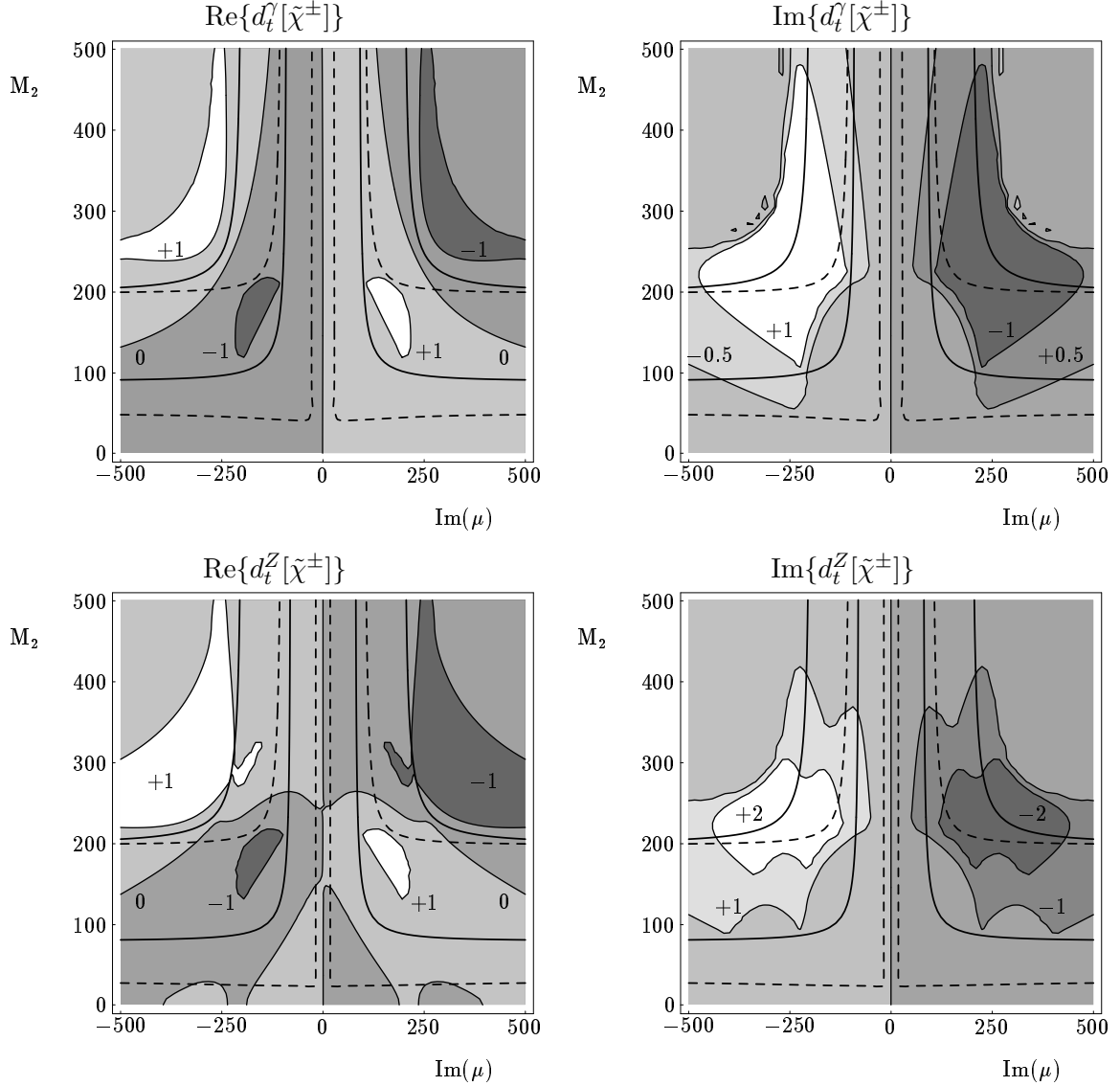


Figure 3: *Chargino contribution to the real and imaginary parts of the t EDFF and WEFF [in $10^{-3}\mu_t$ units] in the plane $M_2 - \text{Im}(\mu)$ for $\tan\beta = 1.6$, $|m_{LR}^b| = 200$ GeV and $\varphi_{\tilde{b}} = \pi/2$ at $\sqrt{s} = 500$ GeV. The lower (upper) solid isolines correspond to $m_{\tilde{\chi}_1^\pm} = 90$ (200) GeV and the dashed isolines to $m_{\tilde{\chi}_1^0} = 25$ (100) GeV.*

4.2.4 Total contribution

In view of these results, we establish a set of SUSY parameters and phases for which nearly all the contributions sum up constructively at $\sqrt{s} = 500$ GeV. Our choice is

$$\begin{aligned} \text{Reference Set \#1 : } \quad & \tan\beta = 1.6 \\ & M_2 = |\mu| = m_{\tilde{q}} = |m_{LR}^t| = |m_{LR}^b| = 200 \text{ GeV} \\ & \varphi_\mu = -\varphi_{\tilde{t}} = -\varphi_{\tilde{b}} = \pi/2, \end{aligned} \tag{26}$$

for which the t EDFF and WEFF reach the values:

$$d_t^\gamma = (1.407 - 1.618 i) \times 10^{-3} \mu_t \tag{27}$$

$$d_t^Z = (0.624 - 2.242 i) \times 10^{-3} \mu_t, \tag{28}$$

at $\sqrt{s} = 500$ GeV. To illustrate how the maximum effects appear we display in Fig. 4 the individual contributions as a function of \sqrt{s} . The masses of the supersymmetric partners in the loops are such that there are threshold enhancements in the vicinity of $\sqrt{s} = 500$ GeV.

5 CP-odd observables

One needs to go beyond the Z peak to produce t quark pairs in e^+e^- collisions and this implies to account for several features. The photon-exchange diagram is no longer suppressed in this regime and therefore one needs to separate the contributions of electromagnetic and weak form factors [45]. Moreover, not only vertex- but also box-diagrams correct the tree level process to one loop. The former corrections are parameterized by the electromagnetic and the weak vertex form factors but the latter demand the introduction of new form factors according to the more general topology of the process. For a realistic theory, one expects that any CP-odd observable will depend not only on the CP-violating effects due to vertex corrections included in the electric and weak-electric dipole form factors but also on possible CP-violating box contributions. This is indeed the case of the supersymmetric models.

We concentrate on supersymmetric CP violating effects in t -pair production at e^+e^- colliders. CP conserving MSSM one-loop contributions to $e^+e^- \rightarrow f\bar{f}$ are discussed in [46]. To our knowledge, only the electric and the weak-electric form factors have been considered so far to parameterize these effects.⁸ Our purpose is to evaluate the expectation value of several observables in the context of the MSSM with complex parameters to one loop. Eventually we compare the contribution from the electric and weak-electric form factors to these observables with the CP-violation effects coming from the box contributions.

Our starting point is an initial CP-even eigenstate in the c.m.s. (laboratory frame). This is the case for unpolarized e^+ and e^- beams but only a good approximation in the case of

⁸A similar analysis for hadron colliders has been recently presented in Ref. [47].

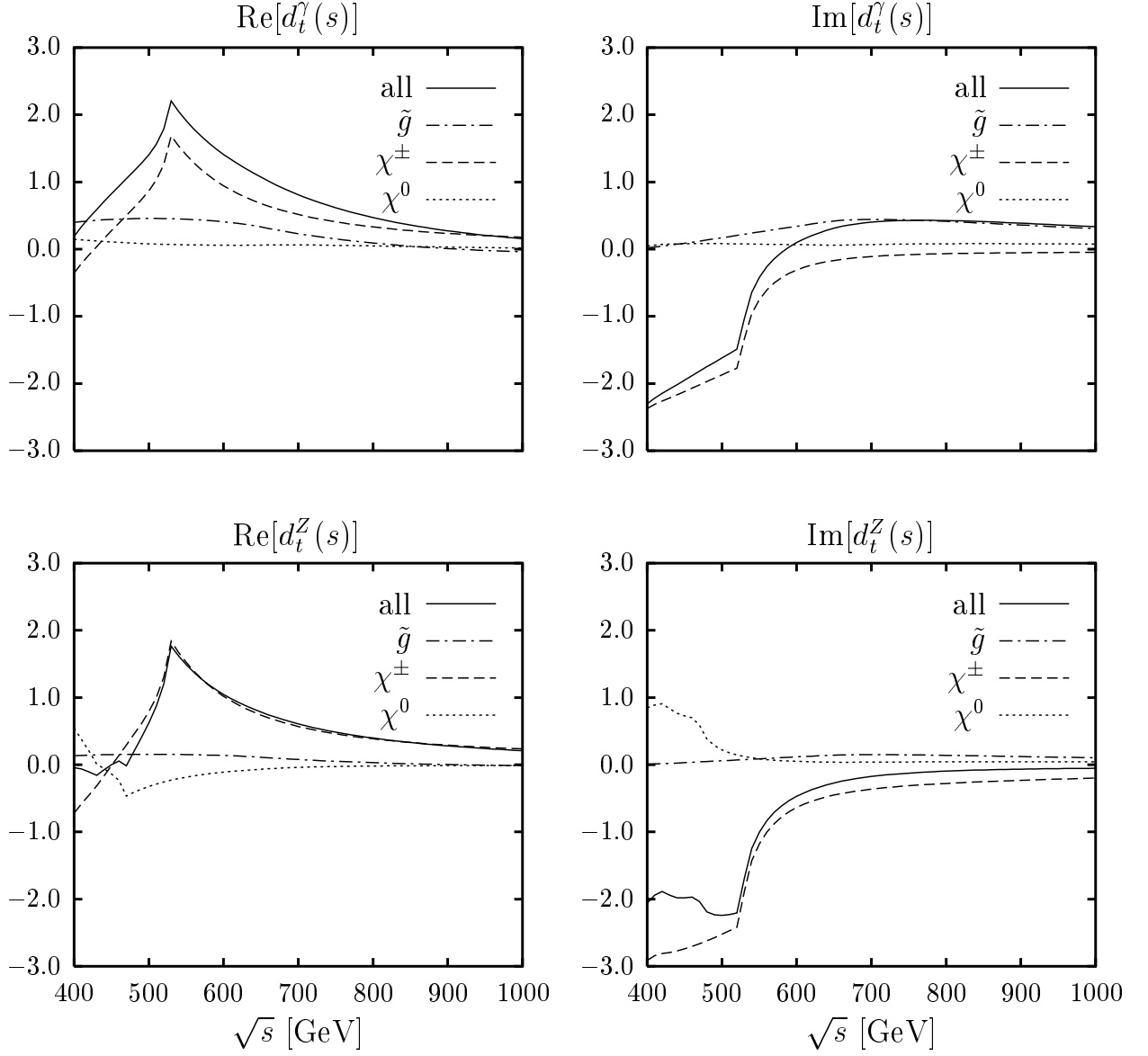


Figure 4: The different contributions to the t (W)EDFF [in $10^{-3}\mu_t$ units] for the reference set of SUSY parameters of Eq. (26).

longitudinally polarized beams [48] (unless they are ideally 100% polarized): neglecting the electron mass, chirality conservation allows only interactions of equal helicity states that project into each other under a CP transformation.

Consider the process $e^+(\mathbf{p}_+) + e^-(\mathbf{p}_-) \rightarrow t(\mathbf{k}_+, \mathbf{s}_1) + \bar{t}(\mathbf{k}_-, \mathbf{s}_2)$ (pair-production of polarized t quarks). The decay channels labeled by a and c act as spin analyzers in $t + \bar{t} \rightarrow a(\mathbf{q}_+) + \bar{c}(\mathbf{q}_-) + X$. The momenta and polarization vectors in the overall c.m.s. transform under CP and CPT as follows:⁹

$$\begin{array}{ll}
\text{CP : } \mathbf{p}_\pm \rightarrow -\mathbf{p}_\mp = \mathbf{p}_\pm & \text{CPT : } \mathbf{p}_\pm \rightarrow \mathbf{p}_\mp = -\mathbf{p}_\pm \\
\mathbf{k}_\pm \rightarrow -\mathbf{k}_\mp = \mathbf{k}_\pm & \mathbf{k}_\pm \rightarrow \mathbf{k}_\mp = -\mathbf{k}_\pm \\
\mathbf{q}_\pm \rightarrow -\mathbf{q}_\mp & \mathbf{q}_\pm \rightarrow \mathbf{q}_\mp \\
\mathbf{s}_1 \leftrightarrow \mathbf{s}_2 & \mathbf{s}_1 \leftrightarrow -\mathbf{s}_2
\end{array} \tag{29}$$

From the unit momentum of one of the t quarks in the c.m.s. (say $\hat{\mathbf{k}}_+$) and their polarizations ($\mathbf{s}_1, \mathbf{s}_2$) a basis of linearly independent CP-odd *spin observables* can be constructed [45]. They are classified according to their CPT parity. The spin observables are related to more realistic (directly measurable) *momentum observables* based on the momenta of the top decay products [49]. The polarizations can be analyzed through the angular correlation of the weak decay products, both in the nonleptonic and in the semileptonic channels:

$$t(\mathbf{k}_+) \rightarrow b(\mathbf{q}_b)X_{\text{had}}(\mathbf{q}_x) , \tag{30}$$

$$t(\mathbf{k}_+) \rightarrow b(\mathbf{q}_b)\ell^+(\mathbf{q}_+)\nu_\ell \quad (\ell = e, \mu, \tau) \tag{31}$$

and the charged conjugated ones.¹⁰ As $m_t > M_W + m_b$, the t quark decays proceed predominantly through Wb . Within the SM the angular distribution of the charged lepton is a much better spin analyzer of the t quark than that of the b quark or the W boson arising from semileptonic or nonleptonic t decays [51]. The dimensionless observables are easier to measure, for instance the scalar CP-odd observables [45]:

$$\hat{A}_1 \equiv \hat{\mathbf{p}}_+ \cdot \frac{\hat{\mathbf{q}}_+ \times \hat{\mathbf{q}}_-}{|\hat{\mathbf{q}}_+ \times \hat{\mathbf{q}}_-|} \quad [\text{CPT-even}] \tag{32}$$

$$\hat{A}_2 \equiv \hat{\mathbf{p}}_+ \cdot (\hat{\mathbf{q}}_+ + \hat{\mathbf{q}}_-) \quad [\text{CPT-odd}] \tag{33}$$

or the CP-odd traceless tensors [45]:

$$\hat{T}_{ij} \equiv (\hat{\mathbf{q}}_+ - \hat{\mathbf{q}}_-)_i \frac{(\hat{\mathbf{q}}_+ \times \hat{\mathbf{q}}_-)_j}{|\hat{\mathbf{q}}_+ \times \hat{\mathbf{q}}_-|} + (i \leftrightarrow j) \quad [\text{CPT-even}] \tag{34}$$

$$\hat{Q}_{ij} \equiv (\hat{\mathbf{q}}_+ + \hat{\mathbf{q}}_-)_i (\hat{\mathbf{q}}_+ - \hat{\mathbf{q}}_-)_j + (i \leftrightarrow j) \quad [\text{CPT-odd}] \tag{35}$$

⁹T means reflection of spins and momenta.

¹⁰The leading QCD corrections to $e^+e^- \rightarrow t\bar{t}$, that include a gluon emission, have a very small effect on the t spin orientation [50].

The reconstruction of the t frame is not necessary for the momentum observables. The observables \hat{A}_2 and \hat{Q}_{ij} do not involve angular correlations as they could be measured considering separate samples of events in the reactions $e^+e^- \rightarrow aX$ and $e^+e^- \rightarrow \bar{a}X$. Nevertheless it is convenient to treat them in an event-by-event basis [45].

One may obtain additional CP-odd observables from combinations of the standard tensors by multiplying them with CP-even scalar weight functions to maximize the sensitivity to CP-violating effects (*optimal observables*). Neglecting quartic terms in the CP-violating form factors, λ_i , the differential cross section can be written as $d\sigma = d\sigma_0 + \sum_i \lambda_i d\sigma_1^i$. It has been shown that the observables given by $\mathcal{O}_i = d\sigma_1^i/d\sigma_0$ have maximal sensitivity to the CP-violating terms λ_i [52]. The CP-odd and CPT-even (odd) observables are sensitive to the dispersive (absorptive) parts of the CP-violating form factors. These include the real (imaginary) parts of the electric and weak-electric dipole form factors as well as CP-violating contributions from box topologies.

Since the t quark is a heavy fermion, the CP conjugate modes $t_L\bar{t}_L$ and $t_R\bar{t}_R$ are produced with a sizeable rate. This allows to construct the following CP-odd asymmetry [53, 31]

$$A = \frac{\#(t_L\bar{t}_L) - \#(t_R\bar{t}_R)}{\#(t_L\bar{t}_L) + \#(t_R\bar{t}_R)} \quad [\text{CPT-odd}] \quad (36)$$

This asymmetry is related to the one that can be measured through the energy spectra of prompt leptons in the decays $t \rightarrow W^+b \rightarrow \ell^+\nu_\ell b$ and its conjugate. The W^+ is predominantly longitudinally polarized and, assuming the standard $V-A$ interaction, the b quark is preferentially left-handed. The W^+ is mostly collinear with the t polarization and so is the ℓ^+ anti-lepton. Above the $t\bar{t}$ threshold a ℓ^+ coming from a t_R has more energy, due to the Lorentz boost, than one produced in a t_L decay. The same happens for the conjugate channel, the ℓ^- from a \bar{t}_L is in average more energetic than the one from the \bar{t}_R . Therefore, in the decay of the $t_R\bar{t}_R$ the anti-lepton from t_R has a higher energy E_+ , while in the decay of the pair $t_L\bar{t}_L$ the lepton from \bar{t}_L has a higher energy E_- . Thus the asymmetry A is sensitive to the energy asymmetry of the leptons [54] or b quarks [55] in the final state.

We will ignore possible CP violation in the t or \bar{t} decays. CP-violating t decays in supersymmetry have been considered in [56]. We evaluate the influence on the CP-odd observables of the vertex and box diagrams through (ideal) spin observables. The expectation value of the realistic momentum observables given above will also be presented (assuming SM top decays) for comparison with experimental capabilities.

6 MSSM full contribution to CP-odd observables

The one-loop differential cross section for polarized t -pair production in the MSSM [46] involves the box diagrams indicated in Fig. 5 besides the vertex graphs of Fig. 1. The class with vector boson exchange contains only SM contributions ($[eZZt]$, $[\nu_e WWb]$) whereas the

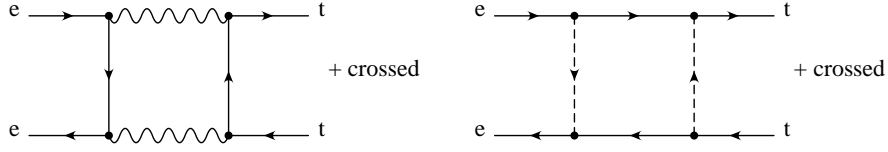


Figure 5: *Relevant generic box graphs for the MSSM at one loop.*

Table 2: *CP-odd spin observables and the coefficients for the expectation value of their integrated version at $\sqrt{s} = 500$ GeV, where only the CP-violating dipole form factors are taken into account.*

i	CPT	\mathcal{O}_i	\mathbf{a}	\mathbf{b}	c_1	c_2	c_3	c_4
1	even	$(\mathbf{s}_1^* - \mathbf{s}_2^*)_y$	T \uparrow	T \downarrow	0.526	0	1.517	0
2	even	$(\mathbf{s}_1^* \times \mathbf{s}_2^*)_x$	T \uparrow	L \uparrow	-0.465	0	-0.061	0
3	even	$(\mathbf{s}_1^* \times \mathbf{s}_2^*)_z$	N \uparrow	T \uparrow	0.708	0	0.144	0
4	odd	$(\mathbf{s}_1^* - \mathbf{s}_2^*)_x$	N \uparrow	N \downarrow	0	0.930	0	0.123
5	odd	$(\mathbf{s}_1^* - \mathbf{s}_2^*)_z$	L \uparrow	L \downarrow	0	-1.417	0	-0.287
6	odd	$(\mathbf{s}_1^* \times \mathbf{s}_2^*)_y$	L \uparrow	T \downarrow	0	0.263	0	0.758

other one is purely supersymmetric ($[\tilde{e}\tilde{\chi}^0\tilde{\chi}^0\tilde{t}]$, $[\tilde{\nu}_e\tilde{\chi}^\pm\tilde{\chi}^\pm\tilde{b}]$) and provides CP violating effects. The box diagrams with Higgs boson exchange are proportional to the electron mass and are neglected in the whole calculation (they are CP even in any case). When we refer to one-loop calculation in the following, the QED as well as the standard QCD corrections to the tree level process are excluded: they need real photonic and gluonic corrections to render an infrared finite result and constitute an unnecessary complication as they are CP-even and do not affect qualitatively our conclusions.

6.1 Spin Observables

A list of CP-odd spin observables classified according to their CPT properties is shown in Table 2. Their expectation values as a function of s and the scattering angle of the t quark in the overall c.m. frame are given by

$$\langle \mathcal{O} \rangle_{\mathbf{ab}} = \frac{1}{2d\sigma} \left[\sum_{\mathbf{s}_1^*, \mathbf{s}_2^* = \pm \mathbf{a}, \pm \mathbf{b}} + \sum_{\mathbf{s}_1^*, \mathbf{s}_2^* = \pm \mathbf{b}, \pm \mathbf{a}} \right] d\sigma(\mathbf{s}_1^*, \mathbf{s}_2^*) \mathcal{O}, \quad (37)$$

$$d\sigma = \sum_{\pm \mathbf{s}_1^*, \pm \mathbf{s}_2^*} d\sigma(\mathbf{s}_1^*, \mathbf{s}_2^*). \quad (38)$$

The directions of polarization of t and \bar{t} (\mathbf{a} , \mathbf{b}) are taken normal to the scattering plane (N), transversal (T) or longitudinal (L). They can be either parallel (\uparrow) or antiparallel (\downarrow) to the axes defined by $\hat{z} = \mathbf{k}_+$, $\hat{y} = \mathbf{k}_+ \times \mathbf{p}_+ / |\mathbf{k}_+ \times \mathbf{p}_+|$ and $\hat{x} = \hat{y} \times \hat{z}$. Notice that

$$\langle \mathcal{O}^2 \rangle_{\mathbf{ab}} = \frac{1}{d\sigma} \sum_{\mathbf{s}_1^*, \mathbf{s}_2^* = \pm \mathbf{a}, \pm \mathbf{b}} d\sigma(\mathbf{s}_1^*, \mathbf{s}_2^*) \mathcal{O}^2 \quad (39)$$

and the same for the average of any CP-even quantity. If the information of the t scattering angle is not available one can consider integrated observables

$$\langle \mathcal{O} \rangle_{\mathbf{ab}} = \frac{1}{2\sigma} \left[\sum_{\mathbf{s}_1^*, \mathbf{s}_2^* = \pm \mathbf{a}, \pm \mathbf{b}} + \sum_{\mathbf{s}_1^*, \mathbf{s}_2^* = \pm \mathbf{b}, \pm \mathbf{a}} \right] \sigma(\mathbf{s}_1^*, \mathbf{s}_2^*) \mathcal{O} . \quad (40)$$

The contributions to the CP-odd observables are linear in the t EDFF and WEDFF and in the CP-violating parts of the one-loop box graphs. The shape of the different dipole contributions to these observables is depicted in Fig. 6. The coefficients of the dipoles in the linear expansion of the integrated spin observables,

$$\langle \mathcal{O} \rangle_{\mathbf{ab}} \equiv \frac{2m_t}{e} \left(c_1 \operatorname{Re}[d_t^\gamma] + c_2 \operatorname{Im}[d_t^\gamma] + c_3 \operatorname{Re}[d_t^Z] + c_4 \operatorname{Im}[d_t^Z] \right) , \quad (41)$$

are shown in Table 2 for their integrated version at $\sqrt{s} = 500$ GeV. They are model independent.

In Fig. 7 we compare the contributions of dipoles and boxes to the spin observables, for two reference set of parameters. The first set was given in (26) and is the one that has been shown to enhance the dipole effects. The second one is:

$$\begin{aligned} \text{Reference Set \#2 : } \quad & \tan \beta = 1.6 \\ & M_2 = |\mu| = m_{\tilde{q}} = |m_{LR}^t| = |m_{LR}^b| = 200 \text{ GeV} \\ & \varphi_\mu = \varphi_{\tilde{t}} = \varphi_{\tilde{b}} = \pi/2 , \end{aligned} \quad (42)$$

where, compared to (26), only the CP-violating phases have been changed. The shape of the solid and dashed curves is the same in all cases, as expected. Their different size is due to the contributions to the normalization factors coming from self-energies, A(W)MFFs and other CP-even corrections. The plots show that for the Set #1 the MSSM box graphs contribute (in the case of CPT-even observables) to CP violation in the process $e^+e^- \rightarrow t\bar{t}$ by roughly the same amount and with a different profile than the EDFFs and WEDFF of the MSSM. For nearly all cases this eventually results in a large reduction of the value of any CP-odd observable with respect to the expectations from the dipoles alone, as it will be shown below. Other sets of SUSY parameters, that do not enhance the dipole contributions, can provide instead *smaller dipole form factors but larger observable effects*. This is the case of the Set #2, that yields much smaller values for the real parts of the dipole form factors at $\sqrt{s} = 500$ GeV than we had before in Eq. (28),

$$d_t^\gamma = (0.547 - 1.889 i) \times 10^{-3} \mu_t, \quad (43)$$

$$d_t^Z = (0.362 - 2.319 i) \times 10^{-3} \mu_t. \quad (44)$$

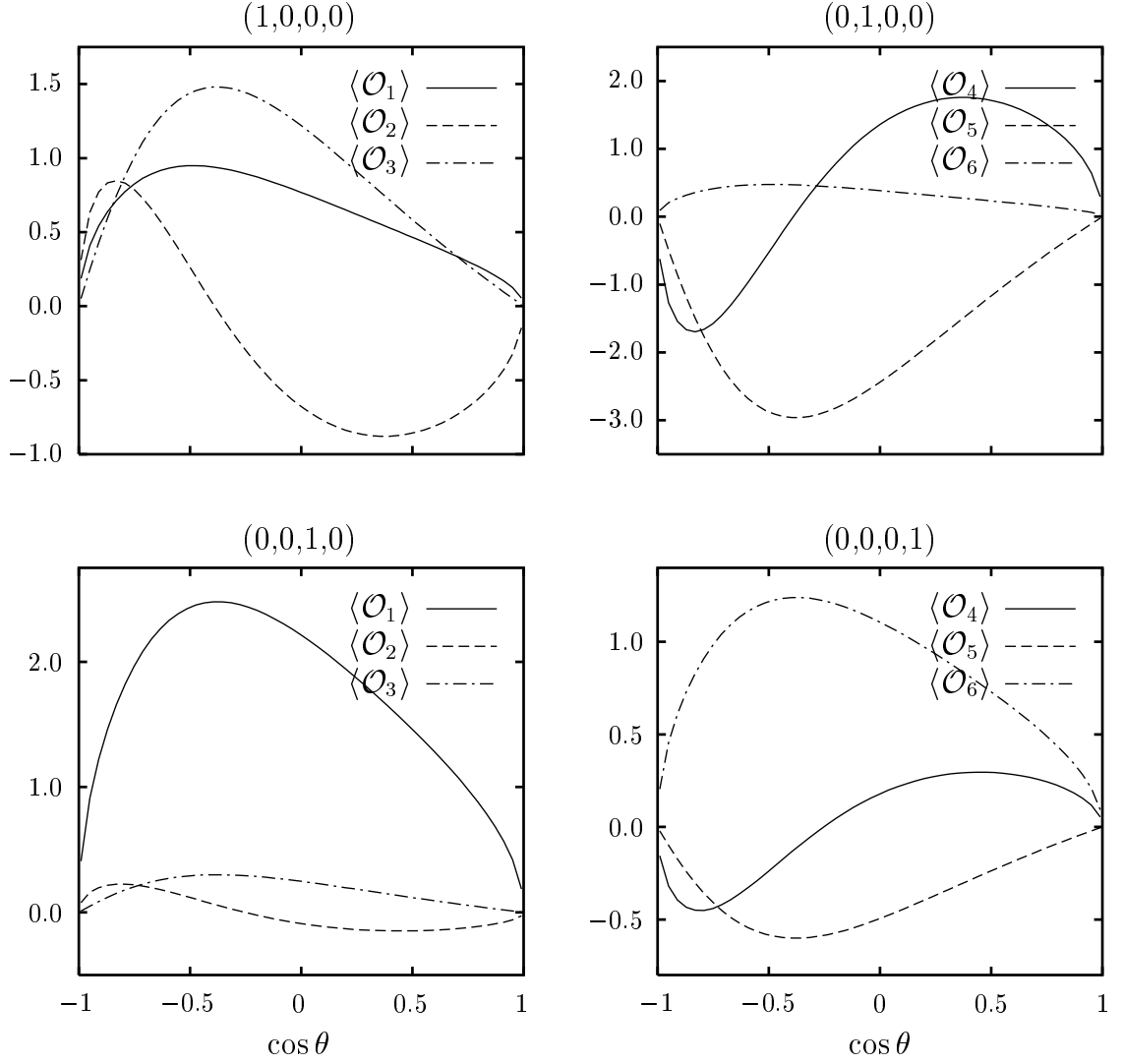


Figure 6: Dipole contributions to the expectation values of the spin observables at $\sqrt{s} = 500$ GeV for different values of $(\text{Re}[d_t^I], \text{Im}[d_t^I], \text{Re}[d_t^Z], \text{Im}[d_t^Z])$ in μ_t units.

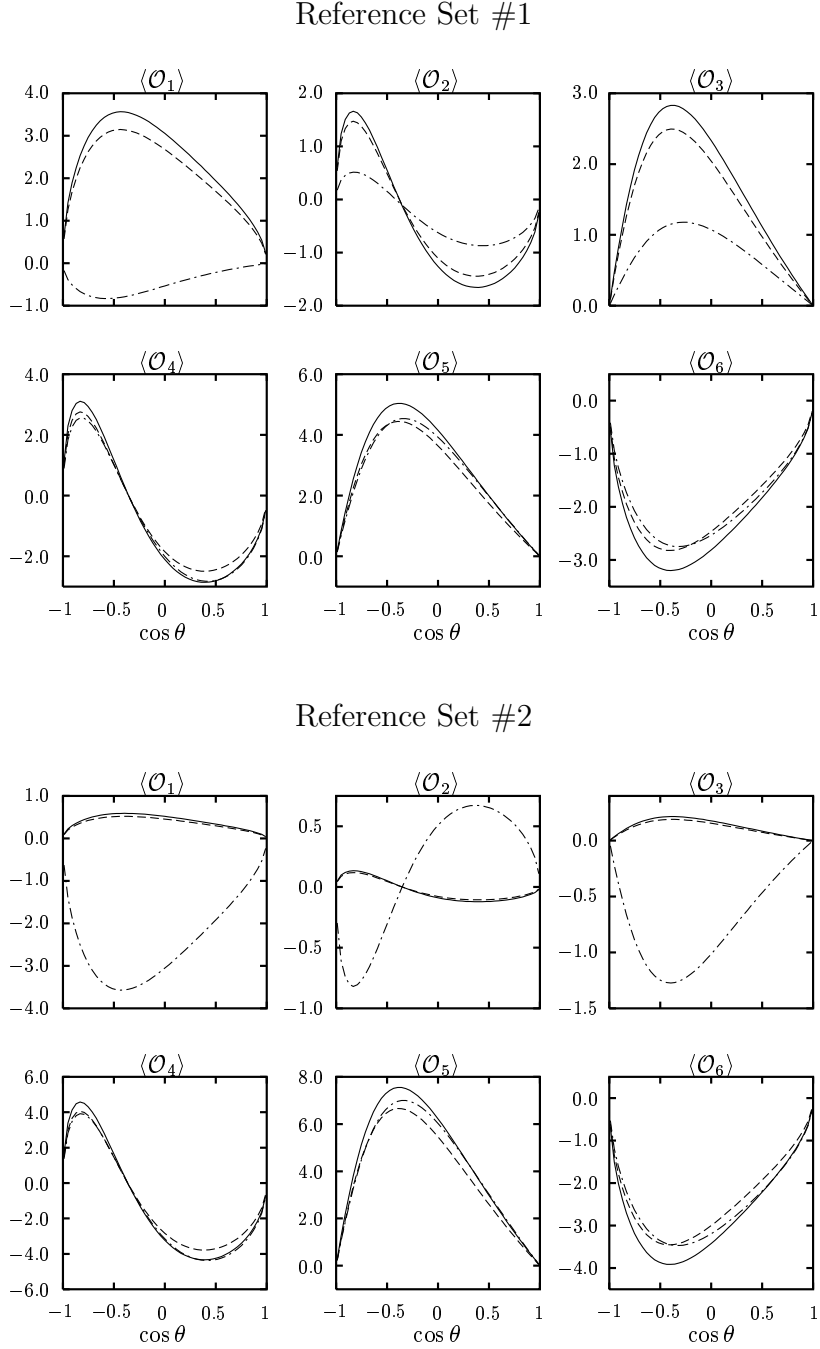


Figure 7: *Expectation value of the spin observables [in 10^{-3} units] for the two reference sets of SUSY parameters, assuming for the cross section: (i) tree level plus contribution from $(W)EDFFs$ only (solid line); (ii) one loop including all the vertex corrections and the self-energies (dashed line); (iii) complete one loop (dot-dashed line).*

Table 3: Ratio $r \equiv \langle \mathcal{O} \rangle / \sqrt{\langle \mathcal{O}^2 \rangle}$ [in 10^{-3} units] of the integrated spin observables at $\sqrt{s} = 500$ GeV for the two reference sets of SUSY parameters. The left column excludes the box corrections and the right one comes from the complete one-loop cross section for $e^+e^- \rightarrow t\bar{t}$.

i	CPT	\mathcal{O}_i	\mathbf{a}	\mathbf{b}	Set #1		Set #2	
1	even	$(\mathbf{s}_1^* - \mathbf{s}_2^*)_y$	T \uparrow	T \downarrow	1.216	-0.231	0.207	-1.394
2	even	$(\mathbf{s}_1^* \times \mathbf{s}_2^*)_x$	T \uparrow	L \uparrow	-0.755	-0.489	-0.053	0.318
3	even	$(\mathbf{s}_1^* \times \mathbf{s}_2^*)_z$	N \uparrow	T \uparrow	1.184	0.625	0.090	-0.598
4	odd	$(\mathbf{s}_1^* - \mathbf{s}_2^*)_x$	N \uparrow	N \downarrow	-1.230	-1.421	-1.888	-2.217
5	odd	$(\mathbf{s}_1^* - \mathbf{s}_2^*)_z$	L \uparrow	L \downarrow	2.550	2.739	3.823	4.216
6	odd	$(\mathbf{s}_1^* \times \mathbf{s}_2^*)_y$	L \uparrow	T \downarrow	-1.683	-1.751	-2.050	-2.216

As a consequence, the CPT-even observables receive their contributions mainly from the box diagrams (Fig. 7) for the Set #2.

The previous arguments are reflected in Table 3 where the ratio $r \equiv \langle \mathcal{O} \rangle / \sqrt{\langle \mathcal{O}^2 \rangle}$ is shown for the integrated spin observables. We compare the result when only the self energies and vertex corrections are included (left column) with the complete one-loop calculation (right column). The shape of the observables as a function of the t polar angle (Fig. 7) is such that signal for CP-violation r is still not very large for a couple of CPT-even observables with the Set #2 but it is much better for all the others. This illustrates that the dipole form factors of the t quark are not sufficient to parameterize observable CP-violating effects and the predictions can be wrong by far.

As a final remark, note that $\langle \mathcal{O}_5 \rangle = A$, the asymmetry defined in Eq. (36). Attending to Table 2 it happens to be the most sensitive observable to the imaginary part of the EDFF and also the best one to test CP violation for our choice of SUSY parameters (Table 3). The observables $(\mathbf{s}_1^* - \mathbf{s}_2^*)$ can still give information on CP violation when the polarization of one of the t quarks is not analyzed.¹¹ The sensitivity of the single-spin polarization to CP-violation is indeed worse: $\langle (\mathbf{s}_1^* - \mathbf{s}_2^*)_{x,y,z} \rangle_{\mathbf{ab}} = 2 \langle (\mathbf{s}_1^*)_{x,y,z} \rangle_{\mathbf{a}}$ for $\mathbf{a}(\mathbf{b}) = \text{N}\uparrow(\downarrow), \text{T}\uparrow(\downarrow), \text{L}\uparrow(\downarrow)$.

6.2 Momentum Observables

Consider now the decay channels labeled by a and c acting as spin analyzers in $t + \bar{t} \rightarrow a(\mathbf{q}_+) + \bar{c}(\mathbf{q}_-) + X$. The expectation value of a CP-odd observable is given by the average

¹¹Anyway a comparison between two samples, one with polarized t and the other with polarized \bar{t} , is necessary to build the genuine CP-odd observable of Eq. (38).

Table 4: Ratio r [in 10^{-3} units] of the momentum observables (32–35) at $\sqrt{s} = 500$ GeV for three different channels: $t + \bar{t} \rightarrow a(\mathbf{q}_+) + \bar{c}(\mathbf{q}_-) + X$, given the Set #2 of SUSY parameters (42). The left column includes only the t (W)EDFF corrections and the right one comes from the complete one-loop cross section for $e^+e^- \rightarrow t\bar{t}$.

CPT	\mathcal{O}	$b - b$		$\ell - b$		$\ell - \ell$	
even	\hat{A}_1	-0.036	0.242	0.030	-0.202	0.068	-0.467
odd	\hat{A}_2	0.270	0.304	-0.180	-0.204	-0.501	-0.812
even	\hat{T}_{33}	-0.006	0.042	0.021	-0.140	-0.037	0.248
odd	\hat{Q}_{33}	0.486	0.542	-0.335	-0.374	-1.274	-1.420

over the phase space of the final state particles,

$$\langle \mathcal{O} \rangle_{ac} = \frac{1}{2} [\langle \mathcal{O} \rangle_{a\bar{c}} + \langle \mathcal{O} \rangle_{c\bar{a}}] = \frac{1}{2\sigma_{ac}} \int [d\sigma_{a\bar{c}} + d\sigma_{c\bar{a}}] \mathcal{O} , \quad (45)$$

where both the process $(a\bar{c})$ and its CP conjugate $(c\bar{a})$ are included and

$$\sigma_{ac} = \int d\sigma_{a\bar{c}} = \int d\sigma_{c\bar{a}} , \quad (46)$$

in full analogy with Eqs. (37,38). The differential cross section for t -pair production and decay is evaluated for every channel using the narrow width approximation.

In Table 4 the ratio r is shown for three different decay channels at $\sqrt{s} = 500$ GeV and some *realistic* CP-odd observables involving the momenta of the decay products analyzing t and \bar{t} polarizations in the laboratory frame. The leptonic decay channels are the best t spin analyzers but the number of leptonic events is also smaller. The Reference Set #2 has been chosen. As expected, the dipole contributions (left columns) to the CPT even observables are very small for this choice of SUSY parameters but the actual expectation values (right columns) are larger.

The previous results were obtained for unpolarized electron and positron beams. Let P_{\pm} be the degree of longitudinal polarization of the initial e^{\pm} . The differential cross section reads now

$$d\sigma = \frac{1}{4} [(1 + P_+)(1 + P_-) d\sigma_R + (1 - P_+)(1 - P_-) d\sigma_L] , \quad (47)$$

where $\sigma_{R/L}$ corresponds to the cross section for electrons and positrons with equal right/left-handed helicity. Chirality conservation suppresses opposite helicities. Table 5 summarizes some extreme cases. If both beams are fully polarized, $P_+ = P_- = \pm 1$, the ratio r is the same as for $(P_{\pm} = 0, P_{\mp} = \pm 1)$, respectively (Table 5), but the cross sections are twice as much

Table 5: *The same as in Table 4 assuming the complete one-loop cross section for $e^+e^- \rightarrow t\bar{t}$ and longitudinal polarizations for one of the e^\pm beams, P_\pm .*

$P_\pm = 0, P_\mp = -1; \sigma_{t\bar{t}} = 0.707 \text{ pb}$				$P_\pm = 0, P_\mp = +1; \sigma_{t\bar{t}} = 0.355 \text{ pb}$			
\mathcal{O}	$b - b$	$\ell - b$	$\ell - \ell$	\mathcal{O}	$b - b$	$\ell - b$	$\ell - \ell$
\hat{A}_1	0.359	-0.298	-0.667	\hat{A}_1	0.016	-0.009	-0.053
\hat{A}_2	0.397	-0.254	-0.952	\hat{A}_2	0.134	-0.099	-0.468
\hat{T}_{33}	0.065	-0.214	0.383	\hat{T}_{33}	-0.003	0.006	-0.020
\hat{Q}_{33}	0.708	-0.488	-1.848	\hat{Q}_{33}	0.210	-0.145	-0.555

(47), which results in a higher statistical significance of the CP signal. From comparison of Table 4 (right columns) with Table 5 is clear that left-handed polarized beams enhance the sensitivity to CP-violating effects.

Concerning the experimental reach of this analysis, the statistical significance of the signal of CP violation is given by $S = |r|\sqrt{N}$ with $N = \epsilon\mathcal{L}\sigma_{t\bar{t}}\text{BR}(t \rightarrow a)\text{BR}(\bar{t} \rightarrow \bar{c})$ where ϵ is the detection efficiency and \mathcal{L} the integrated luminosity of the collider. The branching ratios of the t decays are $\text{BR} \simeq 1$ for the b channel and $\text{BR} \simeq 0.22$ for the leptonic channels ($\ell = e, \mu$). At $\sqrt{s} = 500 \text{ GeV}$ the total cross section for t -pair production is $\sigma_{t\bar{t}} \simeq 0.5 \text{ pb}$ and the NLC integrated luminosity $\mathcal{L} \simeq 50 \text{ fb}^{-1}$ [21]. Assuming a perfect detection efficiency, one gets $\sqrt{N} \simeq 160, 75, 35$ for the channels $b - b, \ell - b, \ell - \ell$, respectively. With these statistics, values of $|r| \sim 10^{-2}$ would be necessary to achieve a 1 s.d. effect, which does not seem to be at hand in the context of the MSSM, even for polarized beams, as Tables 4 and 5 show.

7 Summary and conclusions

The one-loop expressions of the dipole form factors of fermions in terms of arbitrary complex couplings in a general renormalizable theory for the 't Hooft-Feynman gauge have been given. The CP-violating (-conserving) dipole form factors depend explicitly on the imaginary (real) part of combinations of the couplings.

As an application, the electric and the weak-electric dipole form factors of the t quark (for $s > 4m_t^2$) have been evaluated for the MSSM with preserved R-parity and non-universal soft-breaking terms. A version with complex couplings of the MSSM has been implemented in order to get one-loop CP-violating effects. The results depend on three physical CP phases. The supersymmetric parameter space has been scanned in search for the largest contributions to the dipoles. The t dipole form factors are larger in the low $\tan\beta$ scenario. The values depend strongly on the interplay between the energy at which they are evaluated

and the set of supersymmetric parameters used as inputs. The real and imaginary parts can reach values of similar size: at $\sqrt{s} = 500$ GeV, the t EDFF and WEDFF are of $\mathcal{O}(10^{-19})$ ecm.

Away from the Z peak both the electromagnetic and the weak dipole form factors are equally relevant but not enough to parameterize all the physical effects (in particular CP-violation). The case of t -pair production in high energy e^+e^- colliders has been considered to illustrate this fact. Taking several CP-odd spin-observables based on the t and \bar{t} polarization vectors, the different contributions from vertex and box corrections have been evaluated. There is no one loop contribution from the SM sector. It has been shown that, for the set of supersymmetric parameters that provides sizeable values of the t CP-violating dipoles, the SUSY box contributions happen to contribute with opposite sign and in a similar magnitude, yielding altogether a much smaller CP-violating observable effect. Another configuration has been shown for which the dipoles are smaller but the combined effect is larger. The same analysis has been performed using instead realistic observables based on the momenta of t and \bar{t} decay products, with similar results. The channels in which bb , $b\ell$ and $\ell\ell$ act as spin analyzers have been used under the assumption of standard CP-conserving decays and using the narrow width approximation. As expected, the leptons are the best t spin analyzers yielding the maximal values for the signal of CP-violation, $r \simeq 0.5 \times 10^{-3}$. Nevertheless the statistics for such events is smaller.

Acknowledgements

We wish to thank T. Hahn for very valuable assistance in the optimization of the computer codes and the preparation of the figures. Useful discussions with J. Bernabéu and A. Masiero are also gratefully acknowledged. One of us (S.R.) would like to thank the INFN Theoretical Group of Padua for the nice and fruitful hospitality enjoyed during the preparation of part of this paper. S.R. has been supported by the EC under contract ERBFMBICT972474. J.I.I. was supported by the Fundación Ramón Areces at the Karlsruhe U., where most of this work has been carried out, and partially by the Spanish CICYT under contract AEN96-1672.

A Decomposition of the one-loop 3-point integrals

The systematic way of dealing with one-loop integrals consists of reducing the tensor integrals to scalar ones. We employ the following set of 3-point tensor integrals (see Fig. 8):

$$C_{\{0, \mu, \mu\nu\}}(p_1, p_2, M_1, M_2, M_3) \equiv \frac{16\pi^2}{i} \mu^{4-D} \int \frac{d^D l}{(2\pi)^D} \frac{\{1, l_\mu, l_\mu l_\nu\}}{\mathcal{D}_1 \mathcal{D}_2 \mathcal{D}_3}, \quad (48)$$

with

$$\mathcal{D}_1 = (l - p_1)^2 - M_1^2 + i\epsilon,$$

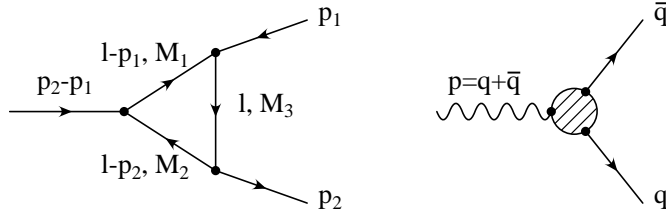


Figure 8: *Momentum convention for 3-point integrals.*

$$\begin{aligned}\mathcal{D}_2 &= (l - p_2)^2 - M_2^2 + i\epsilon, \\ \mathcal{D}_3 &= l^2 - M_3^2 + i\epsilon.\end{aligned}\quad (49)$$

and the orthogonal reduction ($k_{\pm} = p_1 \pm p_2$) [57],

$$C_{\mu} \equiv C_1^+ k_{+\mu} + C_1^- k_{-\mu}, \quad (50)$$

$$C_{\mu\nu} \equiv C_2^+ k_{+\mu} k_{+\nu} + C_2^- k_{-\mu} k_{-\nu} + C_2^{+-} [k_{+\mu} k_{-\nu} + k_{+\nu} k_{-\mu}] + C_2^0 g_{\mu\nu}. \quad (51)$$

This decomposition is very convenient because the integral (48) is invariant under the combined replacements $p_1 \leftrightarrow p_2$ and $M_1 \leftrightarrow M_2$, and we are dealing with equal mass final-state particles $p_1^2 = p_2^2 = m^2$. Therefore C_1^- and C_2^{+-} are antisymmetric under these replacements while the other scalar integrals are symmetric, and the case $M_1 = M_2$ automatically yields $C_1^- = C_2^{+-} = 0$.

For comparison we also list the tensor decomposition defined in [58].

$$C_{\{0, \mu, \mu\nu\}}^{(D)}(p_1, p_2, M_3, M_1, M_2) \equiv \frac{16\pi^2}{i} \mu^{4-D} \int \frac{d^D l}{(2\pi)^D} \frac{\{1, l_{\mu}, l_{\mu} l_{\nu}\}}{\mathcal{D}_1 \mathcal{D}_2 \mathcal{D}_3}, \quad (52)$$

with

$$\begin{aligned}\mathcal{D}_1 &= l^2 - M_3^2 + i\epsilon, \\ \mathcal{D}_2 &= (l + p_1)^2 - M_1^2 + i\epsilon, \\ \mathcal{D}_3 &= (l + p_2)^2 - M_2^2 + i\epsilon.\end{aligned}\quad (53)$$

and the tensor decomposition

$$C_{\mu}^{(D)} \equiv p_{1\mu} C_1^{(D)} + p_{2\mu} C_2^{(D)}, \quad (54)$$

$$C_{\mu\nu}^{(D)} \equiv g_{\mu\nu} C_{00}^{(D)} + p_{1\mu} p_{1\nu} C_{11}^{(D)} + p_{2\mu} p_{2\nu} C_{22}^{(D)} + (p_{1\mu} p_{2\nu} + p_{1\nu} p_{2\mu}) C_{12}^{(D)}. \quad (55)$$

These scalar integrals are related to the ones obtained by orthogonal reduction in the following way:

$$C_1^{(D)} = -C_1^+ - C_1^-, \quad (56)$$

$$C_2^{(D)} = -C_1^+ + C_1^-, \quad (57)$$

$$C_{00}^{(D)} = C_2^0, \quad (58)$$

$$C_{11}^{(D)} = C_2^+ + C_2^- + 2C_2^{+-}, \quad (59)$$

$$C_{22}^{(D)} = C_2^+ + C_2^- - 2C_2^{+-}, \quad (60)$$

$$C_{12}^{(D)} = C_2^+ - C_2^-, \quad (61)$$

with the arguments

$$C_i^{(D)} = C_i^{(D)}(p_1, p_2, M_3, M_1, M_2), \quad C_i^j = C_i^j(-p_1, -p_2, M_1, M_2, M_3).$$

B Conventions for fields and couplings in the SM and the MSSM

B.1 The conventions

We use the conventions of Ref. [59]. The covariant derivative acting on a $SU(2)_L$ weak doublet field with hypercharge Y is given by

$$D_\mu = \partial_\mu + ig \frac{\tau^a}{2} W_\mu^a + ig' \frac{Y}{2} B_\mu, \quad (62)$$

where τ^a are the usual Pauli matrices and the electric charge operator is $Q_f = I_3^f + Y/2$, with $I_3^f = \tau^3/2$. The Z and photon fields are defined by

$$Z_\mu = W_\mu^3 \cos \theta_W - B_\mu \sin \theta_W, \quad (63)$$

$$A_\mu = W_\mu^3 \sin \theta_W + B_\mu \cos \theta_W. \quad (64)$$

The charged weak boson field is $W_\mu^\pm = \frac{1}{\sqrt{2}}(W_\mu^1 \mp iW_\mu^2)$.

In the Standard Model (SM), there is only one Higgs doublet \mathbf{H} with hypercharge $Y = 1$. After spontaneous symmetry breaking (SSB), the physical Higgs field H^0 and the would-be-Goldstone bosons χ and ϕ^\pm are given by

$$\mathbf{H} = \begin{pmatrix} \phi^+ \\ \frac{1}{\sqrt{2}}[v + H^0 + i\chi] \end{pmatrix}. \quad (65)$$

In the Minimal Supersymmetric Standard Model (MSSM) there are the same matter and gauge field multiplets as in the SM, each supplemented by superpartner fields to make up complete supersymmetry multiplets. The matter and gauge fields have the same quantum number assignments as in the SM. But in the MSSM there are two Higgs doublets with opposite hypercharges. Each forms a chiral supersymmetry multiplet and an $SU(2)$ doublet. The

Lagrangian we use is defined in Ref. [60], especially in Eq. (1.45) and Eq. (1.54). We do not impose any reality constraint onto the parameters except for the reality of the Lagrangian.

Spontaneous breakdown of the $SU(2) \times U(1)$ gauge symmetry leads to the existence of five physical Higgs particles: two CP-even Higgs bosons h and H , a CP-odd or pseudoscalar Higgs boson A , and two charged Higgs particles H^\pm . They are grouped in two doublets, $\mathbf{H}_1 \equiv i\tau^2 \Phi_1^*$ and $\mathbf{H}_2 \equiv \Phi_2$, with opposite hypercharges ($Y = \mp 1$), where

$$\Phi_1 = \begin{pmatrix} \phi_1^+ \\ \phi_1^0 \end{pmatrix}, \quad \Phi_2 = \begin{pmatrix} \phi_2^+ \\ \phi_2^0 \end{pmatrix}. \quad (66)$$

After SSB these are expressed in terms of the physical fields h, H, A, H^\pm and the would-be-Goldstone bosons G^0, G^\pm by

$$\phi_1^+ = -H^+ \sin \beta + G^+ \cos \beta, \quad (67)$$

$$\phi_1^0 = \frac{1}{\sqrt{2}} \left\{ v_1 + [(-h \sin \alpha + H \cos \alpha) + i(-A \sin \beta + G^0 \cos \beta)] \right\}, \quad (68)$$

$$\phi_2^+ = H^+ \cos \beta + G^+ \sin \beta, \quad (69)$$

$$\phi_2^0 = \frac{1}{\sqrt{2}} \left\{ v_2 + [(h \cos \alpha + H \sin \alpha) + i(A \cos \beta + G^0 \sin \beta)] \right\}. \quad (70)$$

Besides the four masses, two additional parameters are needed to describe the Higgs sector at tree-level: $\tan \beta = v_2/v_1$, the ratio of the two vacuum expectation values, and a mixing angle α in the CP-even sector. However, only two of these parameters are independent. Using M_A and $\tan \beta$ as input parameters, the masses and the mixing angle α in the H, h sector read [59]

$$M_{h,H}^2 = \frac{1}{2}(M_A^2 + M_Z^2 + \epsilon) \times \left[1 \mp \sqrt{1 - 4 \frac{M_A^2 M_Z^2 \cos^2 2\beta + \epsilon(M_A^2 \sin^2 \beta + M_Z^2 \cos^2 \beta)}{(M_A^2 + M_Z^2 + \epsilon)^2}} \right], \quad (71)$$

$$M_{H^\pm} = M_A \left[1 + \frac{M_W^2}{M_A^2} \right]^{1/2}, \quad (72)$$

$$\tan 2\alpha = \tan 2\beta \frac{M_A^2 + M_Z^2}{M_A^2 - M_Z^2 + \epsilon / \cos 2\beta}; \quad -\frac{\pi}{2} < \alpha < 0, \quad (73)$$

which include the leading radiative correction

$$\epsilon = \frac{3G_F}{\sqrt{2}\pi^2} \frac{m_t^4}{\sin^2 \beta} \log \left(1 + \frac{m_{\tilde{q}}^2}{m_t^2} \right). \quad (74)$$

Here G_F is the Fermi constant and $m_{\tilde{q}}$ is the common mass scale for the squarks.

The mass terms for the neutral gauginos and Higgsinos originate from the bilinear Higgs part of the superpotential (the μ term) and the soft-SUSY-breaking gaugino mass terms

with masses M_2 and M_1 for the SU(2) and U(1) gauginos λ^a and λ' , respectively. The gaugino mass parameters are constrained by the GUT relations

$$M_1 = \frac{5}{3} \tan^2 \theta_W M_2, \quad M_3 = \frac{\alpha_s}{\alpha} s_W^2 M_2. \quad (75)$$

Mixing terms arise from the minimal coupling terms between Higgs, Higgsino and gaugino fields, where the Higgs fields have been replaced by their vacuum expectation values. In terms of two-component spinors the mass terms add up to

$$\mathcal{L}_m^{\tilde{\chi}^0} = -\frac{1}{2}(-i\lambda', -i\lambda^3, \psi_{H_1}^0, \psi_{H_2}^0) Y (-i\lambda', -i\lambda^3, \psi_{H_1}^0, \psi_{H_2}^0)^T + h.c., \quad (76)$$

with the symmetric mass matrix

$$Y = \begin{pmatrix} M_1 & \cdot & \cdot & \cdot \\ 0 & M_2 & \cdot & \cdot \\ -M_Z s_W \cos \beta & M_Z c_W \cos \beta & 0 & \cdot \\ M_Z s_W \sin \beta & -M_Z c_W \sin \beta & -\mu & 0 \end{pmatrix}. \quad (77)$$

We define the unitary diagonalization matrix N and the matrix N' , which is often more convenient, by the equations

$$N^* Y N^{-1} = N_{diag}, \quad N' = N \cdot \begin{pmatrix} c_W & -s_W & 0 & 0 \\ s_W & c_W & 0 & 0 \\ 0 & 0 & 1 & 0 \\ 0 & 0 & 0 & 1 \end{pmatrix}. \quad (78)$$

In general the μ parameter may be complex and then the neutralino masses depend also on the phase of μ . The neutralino mass eigenstates are four Majorana spinors $\tilde{\chi}_j^0$ given by

$$\tilde{\chi}_j^0 \equiv (P_L N_{jk} + P_R N_{jk}^*) \tilde{\Psi}_k^0, \quad (79)$$

$$\tilde{\Psi}_k^0 \equiv \left(\begin{pmatrix} -i\lambda' \\ i\bar{\lambda}' \end{pmatrix}, \begin{pmatrix} -i\lambda^3 \\ i\bar{\lambda}^3 \end{pmatrix}, \begin{pmatrix} \psi_{H_1}^0 \\ \bar{\psi}_{H_1}^0 \end{pmatrix}, \begin{pmatrix} \psi_{H_2}^0 \\ \bar{\psi}_{H_2}^0 \end{pmatrix} \right). \quad (80)$$

The mass terms for the charged gaugino and Higgsino have the same origin and, in terms of two-component spinors, read

$$\mathcal{L}_m^{\tilde{\chi}^\pm} = -\frac{1}{2}(\psi^+, \psi^-) \begin{pmatrix} 0 & X^T \\ X & 0 \end{pmatrix} \begin{pmatrix} \psi^+ \\ \psi^- \end{pmatrix},$$

$$X \equiv \begin{pmatrix} M_2 & M_W \sqrt{2} \sin \beta \\ M_W \sqrt{2} \cos \beta & \mu \end{pmatrix}, \quad (81)$$

with the abbreviations

$$\psi_j^+ = (-i\lambda^+, \psi_{H_2}^+), \quad \psi_j^- = (-i\lambda^-, \psi_{H_1}^-). \quad (82)$$

We now define unitary diagonalization matrices U, V by the equation

$$U^* X V^{-1} = M_{diag}. \quad (83)$$

The masses of the charginos are given by

$$m_{\tilde{\chi}_{1,2}^\pm}^2 = \frac{1}{2} \left\{ M_2^2 + |\mu|^2 + 2M_W^2 \mp [(M_2^2 - |\mu|^2)^2 + 4M_W^2 \cos^2 2\beta]^{1/2} \right\} \quad (84)$$

$$+ 4M_W^2 (M_2^2 + |\mu|^2 + 2M_2 \text{Re}(\mu) \sin 2\beta)^{1/2}. \quad (85)$$

The chargino mass eigenstates are two Dirac spinors $\tilde{\chi}_j^\pm$ given by

$$\tilde{\chi}_j^\pm \equiv (P_L V_{jk} + P_R U_{jk}^*) \tilde{\Psi}_k, \quad (86)$$

$$\tilde{\Psi}_k \equiv \left(\begin{pmatrix} -i\lambda^+ \\ i\lambda^- \end{pmatrix}, \begin{pmatrix} \psi_{H_2}^+ \\ \bar{\psi}_{H_1}^- \end{pmatrix} \right). \quad (87)$$

We abbreviate the charge conjugated fields as

$$\tilde{\chi}_i^- \equiv \tilde{\chi}_i^{+C}. \quad (88)$$

The mass terms for the scalar quarks originate from the Yukawa couplings to the Higgs fields (which yield the corresponding quark masses) and the soft-SUSY-breaking squark mass terms and squark-Higgs interactions parameterized by $m_{\tilde{q}_{L/R}}^2$ and A_q , respectively. Moreover there are mass and mixing terms from auxiliary field terms involving one or two Higgs bosons and two squark fields. The resulting mass matrix for the two squarks of flavor q is:

$$\mathcal{M}_q^2 = \begin{pmatrix} m_L^{q^2} + m_q^2 & m_{LR}^{q*} m_q \\ m_{LR}^q m_q & m_R^{q^2} + m_q^2 \end{pmatrix}, \quad (89)$$

where

$$m_L^{q^2} \equiv m_{\tilde{q}_L}^2 + \cos 2\beta (I_3^f - Q_f s_W^2) M_Z^2, \quad (90)$$

$$m_R^{q^2} \equiv m_{\tilde{q}_R}^2 + \cos 2\beta (Q_f s_W^2) M_Z^2 \quad (91)$$

and

$$m_{LR}^q \equiv A_q - \mu^* \{ \cot \beta, \tan \beta \}, \quad (92)$$

for {up, down}-type squarks, respectively.

This hermitian mass matrix is diagonalized by a unitary matrix S^q , so we can write the squark mass eigenstates of flavor q as

$$\begin{aligned} \tilde{q}_1 &= S_{11}^q \tilde{q}_L + S_{12}^q \tilde{q}_R, \\ \tilde{q}_2 &= S_{21}^q \tilde{q}_L + S_{22}^q \tilde{q}_R. \end{aligned} \quad (93)$$

In general, $m_{LR}^q = |m_{LR}^q|e^{i\varphi_{\tilde{q}}}$ is a complex number and S^q may be written as

$$S^q = \begin{pmatrix} e^{i\varphi_{\tilde{q}}/2} \cos \theta_{\tilde{q}} & e^{-i\varphi_{\tilde{q}}/2} \sin \theta_{\tilde{q}} \\ -e^{i\varphi_{\tilde{q}}/2} \sin \theta_{\tilde{q}} & e^{-i\varphi_{\tilde{q}}/2} \cos \theta_{\tilde{q}} \end{pmatrix}. \quad (94)$$

The mass terms of the sleptons arise in the same way as the squark masses. The main difference appears for the sneutrinos: there is only one sneutrino for every generation, $\tilde{\nu}_l$, and hence there is no mixing. Moreover, we cannot add trilinear soft-breaking terms to shift the masses of the sneutrinos, whose value is given just by $m_{\tilde{\nu}}^2 = m_{\tilde{l}}^2 + 1/2 \cos 2\beta M_Z^2$. (See Eq. (90)).

In general, the physical sfermion masses are given by

$$m_{f_{1,2}}^2 = m_f^2 + \frac{1}{2} \left\{ (m_R^{f^2} + m_L^{f^2}) \mp \sqrt{(m_R^{f^2} - m_L^{f^2})^2 + 4m_f^2 |m_{LR}^f|^2} \right\}, \quad (95)$$

independent of the phase of m_{LR}^f .

B.2 Physical Phases in the MSSM with complex couplings

As we do not constrain the parameters of the MSSM to be real, the following parameters may take complex values: the Yukawa couplings, μ , the soft parameters m_{12}^2 , M_1 , M_2 , M_3 and the A parameters. But not all combinations of phases in these parameters lead to different physical results because several phases can be absorbed by redefinitions of the fields. We now describe a procedure to eliminate the unphysical phases. We assume the GUT relation between the M_i , so they have one common phase. The only remaining phases will be chosen to be those of μ , the A parameters and, for three generations, one phase for all the Yukawa couplings (the δ_{CKM}).

Analogous to the Standard Model case, the Yukawa couplings can be changed by redefinitions of the quark superfields in such a way that there remains only one phase for three generations and only real couplings for less than three generations.

Table 6: *The charges n_i for three $U(1)$ symmetries that leave $\mathcal{L}_{\text{MSSM}}$ invariant.*

U(1)	M_i	A	m_{12}^2	μ	H_1	H_2	QU	QD	LE	θ
PQ	0	0	-1	-1	1/2	1/2	-1/2	-1/2	-1/2	0
R_1	-1	-1	0	1	0	0	1	1	1	-1/2

Following [12] we consider two $U(1)$ transformations PQ and R_1 that do not only transform the fields but also the parameters of the MSSM. In table 6 the charges n_i of the various

quantities are displayed with which the Lagrangian $\mathcal{L}_{\text{MSSM}}$ is invariant under the combined multiplications with $e^{i\alpha n_i}$. The first transformation is a Peccei-Quinn symmetry and R_1 is an R symmetry that also transforms the θ variables appearing in the arguments of the superfields in $\mathcal{L}_{\text{MSSM}}$.

Since $\mathcal{L}_{\text{MSSM}}$ is invariant under these transformations, so are the physical predictions of the MSSM. If the parameters M_i , A , m_{12}^2 and μ have the phases φ_M , φ_A , $\varphi_{m_{12}^2}$ and φ_μ , we first apply R_1 with the angle φ_M , then PQ with the angle $\varphi_{m_{12}^2}$ and obtain for an arbitrary observable:

$$\begin{aligned} & \sigma(|\mu|, |A|, |M_i|, |m_{12}^2|, \varphi_\mu, \varphi_A, \varphi_M, \varphi_{m_{12}^2}) \\ = & \sigma(|\mu|, |A|, |M_i|, |m_{12}^2|, \varphi_\mu + \varphi_M, \varphi_A - \varphi_M, 0, \varphi_{m_{12}^2}) \\ = & \sigma(|\mu|, |A|, |M_i|, |m_{12}^2|, \varphi_\mu + \varphi_M - \varphi_{m_{12}^2}, \varphi_A - \varphi_M, 0, 0). \end{aligned} \quad (96)$$

So the physical predictions only depend on the absolute values of the parameters and the phases

$$\phi_A \equiv \arg(AM_i^*), \quad \phi_B \equiv \arg(\mu Am_{12}^{2*}). \quad (97)$$

One can replace these phases by another set where only the μ and the A parameters are complex. In our choice, the phase of A is traded for the phase $\varphi_{\bar{f}}$ of the off-diagonal term in the corresponding sfermion mixing matrix: $m_{LR}^f \equiv A_f - \mu^* \{\cot, \tan\} \beta$ (92). Relaxing universality for the soft-breaking terms, every A_f contains a different CP-violating phase.

B.3 Vertex factors

We employ the notation and conventions of the previous sections. The list of generic vertices is shown in Fig. 9.

B.3.1 Couplings in the SM

Vertex 1: Coupling of electroweak gauge bosons and fermions: $ie\gamma_\mu(V - A\gamma_5)$.

$$\gamma \bar{f} f : V = -Q_f, \quad A = 0, \quad (98)$$

$$Z \bar{f} f : V = -\frac{v_f}{2s_W c_W}, \quad A = -\frac{a_f}{2s_W c_W}, \quad (99)$$

$$W^\pm \bar{f}' f : V = A = -\frac{1}{2\sqrt{2}s_W}, \quad (100)$$

with $v_f \equiv (I_3^f - 2s_W^2 Q_f)$, $a_f \equiv I_3^f$.

Vertex 2: Coupling of gluons and quarks: $-ieg_s \gamma_\mu T_a$.

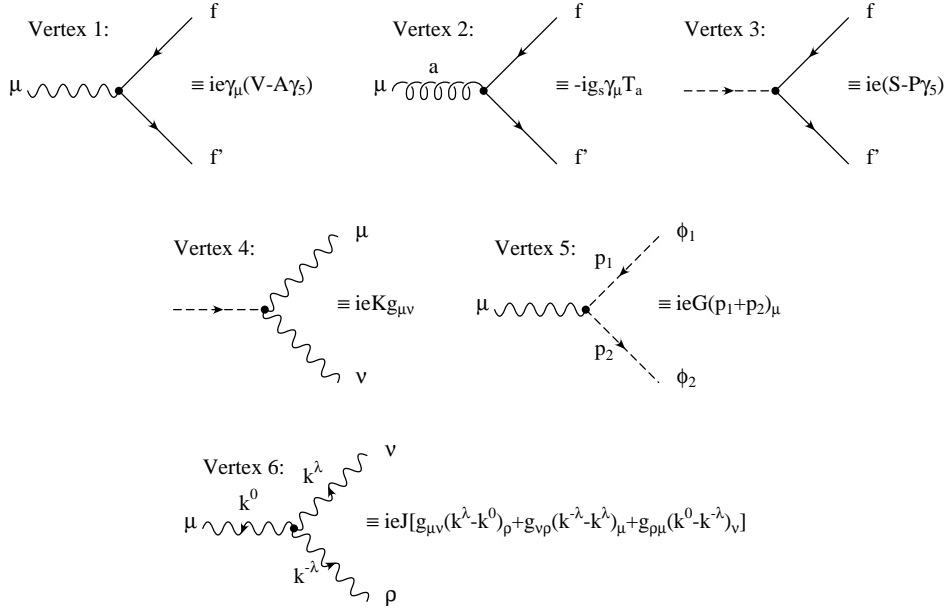


Figure 9: *Generic Vertices.*

Vertex 3: Coupling of two fermions and one Higgs boson ($\mathcal{H}\bar{f}'f$): $ie(S - P\gamma_5)$.

$$H^0\bar{f}'f : \quad S = -\mu_f , \quad P = 0 , \quad (101)$$

$$\chi\bar{f}'f : \quad S = 0 , \quad P = -2iI_3^f\mu_f , \quad (102)$$

$$\phi^\pm\bar{f}'f : \quad S = \sqrt{2}I_3^f[\mu_f - \mu_{f'}] , \quad P = -\sqrt{2}I_3^f[\mu_f + \mu_{f'}] , \quad (103)$$

$$\text{with } \mu_f \equiv \frac{m_f}{2s_W M_W} = \frac{m_f}{2s_W c_W M_Z} .$$

Vertex 4: Coupling of one Higgs boson and two gauge bosons: $ieKg_{\mu\nu}$.

$$H^0ZZ : \quad K = \frac{M_Z}{s_W c_W} , \quad (104)$$

$$H^0W^\pm W^\mp : \quad K = \frac{M_W}{s_W} , \quad (105)$$

$$\phi^\pm W^\mp \gamma : \quad K = M_W , \quad (106)$$

$$\phi^\pm W^\mp Z : \quad K = -M_Z s_W . \quad (107)$$

The rest of the couplings are $K = 0$.

Vertex 5: Coupling of one gauge boson and two Higgs bosons ($V\phi_1\phi_2$): $ieG(p_1 + p_2)_\mu$.

$$\gamma\phi^\lambda\phi^{-\lambda} : \quad G = -\lambda , \quad (108)$$

$$Z\phi^\lambda\phi^{-\lambda} : G = -\lambda\frac{\cos 2\theta_W}{2s_Wc_W}, \quad (109)$$

$$Z\chi H^0 : G = \frac{i}{2s_Wc_W}, \quad (110)$$

$$W^\lambda\phi^{-\lambda}H^0 : G = \frac{\lambda}{2s_W}, \quad (111)$$

$$W^\lambda\phi^{-\lambda}\chi : G = \frac{i}{2s_W}. \quad (112)$$

Interchanging the two Higgs bosons causes the coupling constant to change sign.

Vertex 6: Coupling of three gauge bosons (outgoing momenta):

$$ieJ\{g_{\mu\nu}(k^\lambda - k^0)_\rho + g_{\nu\rho}(k^{-\lambda} - k^\lambda)_\mu + g_{\rho\mu}(k^0 - k^{-\lambda})_\nu\}.$$

$$\gamma W^\lambda W^{-\lambda} : J = -\lambda, \quad (113)$$

$$Z W^\lambda W^{-\lambda} : J = -\lambda\frac{c_W}{s_W}. \quad (114)$$

B.3.2 Couplings in the MSSM

Vertex 1: Coupling of two neutralinos or charginos and one gauge boson: $ie\gamma_\mu(V - A\gamma_5)$.

The fermion flow direction in our Feynman graphs is fixed by the outgoing fermion antifermion pair. The relation between the gauge boson vertex factors for the two different fermion flow directions is obtained by substituting spinors by charge conjugated spinors in the interaction term:

$$V_\mu\tilde{\chi}^+\gamma^\mu(P_Lg_L + P_Rg_R)\tilde{\chi}^+ = V_\mu\tilde{\chi}^-\gamma^\mu(-P_Lg_R - P_Rg_L)\tilde{\chi}^-. \quad (115)$$

Taking into account also the symmetry factor $S = 2$ for the neutralino coupling and $S = 1$ for the charginos, the boson vertex factors $V \equiv (g_L + g_R)/2$ and $A \equiv (g_L - g_R)/2$ are given by:

$$Z\tilde{\chi}_j^0\tilde{\chi}_k^0 : g_L = \frac{1}{2s_Wc_W}(N'_{k4}N'_{j4} - N'_{k3}N'_{j3}), \quad (116)$$

$$g_R = \frac{1}{2s_Wc_W}(N'_{k3}N'_{j3} - N'_{k4}N'_{j4}), \quad (117)$$

$$Z\tilde{\chi}_k^+\tilde{\chi}_j^+ : g_L = -\frac{1}{s_Wc_W}\left[\left(\frac{1}{2} - s_W^2\right)V_{k2}^*V_{j2} + c_W^2V_{k1}^*V_{j1}\right], \quad (118)$$

$$g_R = -\frac{1}{s_Wc_W}\left[\left(\frac{1}{2} - s_W^2\right)U_{k2}U_{j2}^* + c_W^2U_{k1}U_{j1}^*\right], \quad (119)$$

$$Z\tilde{\chi}_k^-\tilde{\chi}_j^- : g_L = \frac{1}{s_Wc_W}\left[\left(\frac{1}{2} - s_W^2\right)U_{k2}U_{j2}^* + c_W^2U_{k1}U_{j1}^*\right], \quad (120)$$

$$g_R = \frac{1}{s_Wc_W}\left[\left(\frac{1}{2} - s_W^2\right)V_{k2}^*V_{j2} + c_W^2V_{k1}^*V_{j1}\right], \quad (121)$$

and

$$\gamma \tilde{\chi}_k^+ \tilde{\chi}_j^+ : g_L = g_R = -\delta_{jk} , \quad (122)$$

$$\gamma \tilde{\chi}_j^- \tilde{\chi}_k^- : g_L = g_R = \delta_{jk} . \quad (123)$$

Vertex 2: There is no genuine supersymmetric vertex of this kind.

Vertex 3: There are three couplings of the kind $i\epsilon(S - P\gamma_5)$:

(Some of the couplings are more easily written in terms of $g_{L,R} \equiv S \pm P$).

- Coupling of one neutralino or chargino to fermions and scalar fermions.

The couplings of neutralinos and charginos to quarks and scalar quarks are given by

$$\mathcal{L}_{\tilde{\chi}q\tilde{q}} = e\tilde{q}^\dagger \tilde{\chi} (P_L g_L + P_R g_R) q + e\bar{q} (P_R g_L^* + P_L g_R^*) \tilde{\chi} \tilde{q} . \quad (124)$$

down-type quarks ($i = 1, 3, 5$):

$$\begin{aligned} \tilde{q}_{i,k}^\dagger \tilde{\chi}_j^0 q_i : g_L = & -\sqrt{2} \left[\left(Q_i N'_{j1} + (I_3^i - Q_i s_W^2) \frac{1}{s_W c_W} N'_{j2} \right) S_{k1}^i \right. \\ & \left. + \frac{m_{q_i}}{2M_W s_W \cos \beta} N'_{j3} S_{k2}^i \right] , \end{aligned} \quad (125)$$

$$\begin{aligned} g_R = & -\sqrt{2} \left[- \left(Q_i N'_{j1} + (-Q_i s_W^2) \frac{1}{s_W c_W} N'_{j2} \right) S_{k2}^i \right. \\ & \left. + \frac{m_{q_i}}{2M_W s_W \cos \beta} N'_{j3} S_{k1}^i \right] , \end{aligned} \quad (126)$$

$$\tilde{q}_{(i+1),k}^\dagger \tilde{\chi}_j^- q_i : g_L = \frac{1}{s_W} \left[-V_{j1}^* S_{k1}^{i+1} + \frac{m_{q_{i+1}}}{\sqrt{2}M_W \sin \beta} V_{j2}^* S_{k2}^{i+1} \right] , \quad (127)$$

$$g_R = \frac{1}{s_W} \left[\frac{m_{q_i}}{\sqrt{2}M_W \cos \beta} U_{j2} S_{k1}^{i+1} \right] . \quad (128)$$

up-type quarks ($i = 2, 4, 6$):

$$\begin{aligned} \tilde{q}_{i,k}^\dagger \tilde{\chi}_j^0 q_i : g_L = & -\sqrt{2} \left[\left(Q_i N'_{j1} + (I_3^i - Q_i s_W^2) \frac{1}{s_W c_W} N'_{j2} \right) S_{k1}^i \right. \\ & \left. + \frac{m_{q_i}}{2M_W s_W \sin \beta} N'_{j4} S_{k2}^i \right] , \end{aligned} \quad (129)$$

$$\begin{aligned} g_R = & -\sqrt{2} \left[- \left(Q_i N'_{j1} + (-Q_i s_W^2) \frac{1}{s_W c_W} N'_{j2} \right) S_{k2}^i \right. \\ & \left. + \frac{m_{q_i}}{2M_W s_W \sin \beta} N'_{j4} S_{k1}^i \right] , \end{aligned} \quad (130)$$

$$\tilde{q}_{(i-1),k}^\dagger \tilde{\chi}_j^+ q_i : g_L = \frac{1}{s_W} \left[-U_{j1}^* S_{k1}^{i-1} + \frac{m_{q_{i-1}}}{\sqrt{2}M_W \cos \beta} U_{j2}^* S_{k2}^{i-1} \right] , \quad (131)$$

$$g_R = \frac{1}{s_W} \left[\frac{m_{q_i}}{\sqrt{2}M_W \sin \beta} V_{j2} S_{k1}^{i-1} \right] . \quad (132)$$

The couplings of neutralinos and charginos to leptons and scalar leptons are given analogously, performing the following substitutions:

$$\begin{aligned}
i = 1, 3, 5 & : \quad \tilde{q}_{i1} \rightarrow \tilde{l}_1, \quad S_{jk}^i \rightarrow S_{jk}^l, \quad Q_i = -1, \quad I_3^i = -\frac{1}{2}, \quad m_{q_i} = m_l, \\
& \quad \tilde{q}_{i2} \rightarrow \tilde{l}_2, \\
i = 2, 4, 6 & : \quad \tilde{q}_{i1} \rightarrow \tilde{\nu}_l, \quad S_{jk}^i \rightarrow \delta_{jk}, \quad Q_i = 0, \quad I_3^i = \frac{1}{2}, \quad m_{q_i} = 0, \\
& \quad \tilde{q}_{i2} \text{ does not exist.}
\end{aligned}$$

- Coupling of one gluino to a quark and a scalar quark.

The interaction between gluinos, quarks and squarks is described by the terms

$$\mathcal{L} = \tilde{q}^\dagger e \bar{g}^a (P_L g_L + P_R g_R) \frac{\lambda^a}{2} q + e \bar{q} (P_R g_L^* + P_L g_R^*) \frac{\lambda^a}{2} \tilde{g}^a \tilde{q}, \quad (133)$$

yielding the vertex factors

$$ie(P_L g_L + P_R g_R) \frac{\lambda^a}{2}, \quad ie(P_R g_L^* + P_L g_R^*) \frac{\lambda^a}{2}. \quad (134)$$

In our calculations the Gell–Mann matrices appear only in the combination

$$\sum_{a=1}^8 \left(\frac{\lambda^a \lambda^a}{4} \right)_{AB} = C_2(F) \delta_{AB} = \frac{4}{3} \delta_{AB}. \quad (135)$$

The couplings are

$$\tilde{q}_i^\dagger \bar{g} q : \quad e g_L = -\sqrt{2} g_s S_{i1}^q, \quad (136)$$

$$e g_R = +\sqrt{2} g_s S_{i2}^q. \quad (137)$$

- Coupling of two fermions and one Higgs boson ($\mathcal{H} \bar{f}' f$).

$$H \bar{u} u : \quad S = -\mu_u \sin \alpha / \sin \beta, \quad P = 0, \quad (138)$$

$$H \bar{d} d : \quad S = -\mu_d \cos \alpha / \cos \beta, \quad P = 0, \quad (139)$$

$$h \bar{u} u : \quad S = -\mu_u \cos \alpha / \sin \beta, \quad P = 0, \quad (140)$$

$$h \bar{d} d : \quad S = \mu_d \sin \alpha / \cos \beta, \quad P = 0, \quad (141)$$

$$A \bar{u} u : \quad S = 0, \quad P = -i \mu_u \cot \beta, \quad (142)$$

$$A \bar{d} d : \quad S = 0, \quad P = -i \mu_d \tan \beta, \quad (143)$$

$$\begin{aligned}
H^+ \bar{u} d : \quad S &= \frac{1}{\sqrt{2}} (\mu_u \cot \beta + \mu_d \tan \beta), \\
P &= \frac{1}{\sqrt{2}} (\mu_u \cot \beta - \mu_d \tan \beta),
\end{aligned} \quad (144)$$

$$G^0 \bar{f}' f : \quad S = 0, \quad P = -2i I_3^f \mu_f, \quad (145)$$

$$G^\pm \bar{f}' f : \quad S = \sqrt{2} I_3^f [\mu_f - \mu_{f'}], \quad P = -\sqrt{2} I_3^f [\mu_f + \mu_{f'}]. \quad (146)$$

with $\mu_f \equiv m_f / 2s_W M_W = m_f / 2s_W c_W M_Z$. For the vertices corresponding to the hermitian conjugated fields we have to replace (S, P) by $(S^*, -P^*)$.

Vertex 4: Coupling of one Higgs boson and two gauge bosons: $ieKg_{\mu\nu}$.

The couplings of a neutral Higgs to two Z bosons are:

$$hZZ : K = \frac{M_Z}{s_W c_W} \sin(\beta - \alpha) , \quad (147)$$

$$HZZ : K = \frac{M_Z}{s_W c_W} \cos(\beta - \alpha) . \quad (148)$$

And the only nonzero couplings of a charged Higgs to neutral gauge and W bosons are:

$$G^\pm W^\mp \gamma : K = M_W , \quad (149)$$

$$G^\pm W^\mp Z : K = -M_Z s_W . \quad (150)$$

The rest of the couplings are $K = 0$.

Vertex 5: There are two types of couplings $Z\phi_1\phi_2$ of the kind $ieG(p_1 + p_2)_\mu$.

- Coupling of two Higgs bosons and one neutral gauge boson.

$$ZAH : G = -\frac{i \sin(\beta - \alpha)}{2s_W c_W} , \quad (151)$$

$$ZAh : G = \frac{i \cos(\beta - \alpha)}{2s_W c_W} , \quad (152)$$

$$ZG^0 H : G = \frac{i \cos(\beta - \alpha)}{2s_W c_W} , \quad (153)$$

$$ZG^0 h : G = \frac{i \sin(\beta - \alpha)}{2s_W c_W} , \quad (154)$$

$$ZH^\lambda H^{-\lambda} : G = -\lambda \frac{\cos 2\theta_W}{2s_W c_W} , \quad (155)$$

$$ZG^\lambda G^{-\lambda} : G = -\lambda \frac{\cos 2\theta_W}{2s_W c_W} , \quad (156)$$

$$\gamma H^\lambda H^{-\lambda} : G = -\lambda , \quad (157)$$

$$\gamma G^\lambda G^{-\lambda} : G = -\lambda . \quad (158)$$

Interchanging the ϕ_1 and ϕ_2 causes the coupling constant to change sign.

- Coupling of two scalar fermions and one neutral gauge boson.

$$\gamma \tilde{q}_{i,j} \tilde{q}_{i,k}^\dagger : G = -Q_i \delta_{jk} , \quad (159)$$

$$Z \tilde{q}_{i,j} \tilde{q}_{i,k}^\dagger : G = -\frac{1}{s_W c_W} \left[(I_3^i - Q_i s_W^2) S_{j1}^{i*} S_{k1}^i - Q_i s_W^2 S_{j2}^{i*} S_{k2}^i \right] . \quad (160)$$

Vertex 6: There is no genuine supersymmetric vertex of this kind.

References

- [1] J. Schwinger, *Phys. Rev.* **D73** (1948) 416.
- [2] Particle Data Group, *Eur. Phys. J.* **C3** (1998) 1.
- [3] T. Kinoshita, B. Nizic, Y. Okamoto, *Phys. Rev.* **D31** (1985) 2108;
T. Kinoshita, W. Marciano, in: *Quantum Electrodynamics*, ed. T. Kinoshita, World Scientific 1990 (p. 419);
J. Bijnens, E. Pallante, J. Prades, *Nucl. Phys.* **B474** (1996) 379, *Phys. Rev. Lett.* **75** (1995) 1447 [E: *Phys. Rev. Lett.* **75** (1995) 3781];
S. Eidelman, F. Jegerlehner, *Z. Phys.* **C67** (1995) 585;
T. Kinoshita, *Phys. Rev. Lett.* **75** (1995) 4728;
A. Czarnecki, B. Krause, W.J. Marciano, *Phys. Rev.* **D52** (1995) 2619, *Phys. Rev. Lett.* **76** (1996) 3267;
F. Jegerlehner, *Nucl. Phys. Proc. Suppl.* **51C** (1996) 131;
S. Laporta, E. Remiddi, *Phys. Lett.* **B379** (1996) 283;
D.H. Brown, W.A. Worstell, *Phys. Rev.* **D54** (1996) 3237;
A. Czarnecki, B. Krause, *Phys. Rev. Lett.* **78** (1997) 4339;
B. Krause, *Phys. Lett.* **B390** (1997) 392;
M. Hayakawa, T. Kinoshita, *Phys. Rev.* **D57** (1998) 465;
M. Davier, A. Höcker, hep-ph/9801361;
G. Degrossi, G.F. Giudice, *Phys. Rev.* **D58** (1998) 053007.
- [4] V. Huges, in *Frontiers of High Energy Spin Physics*, Proceedings of the 10th International Symposium, Nagoya, Japan, edited by T. Hasegawa et al., Universal Academy Press, Tokyo, 1992.
- [5] G. Couture, H. König, *Phys. Rev.* **D53** (1996) 555;
U. Chattopadhyay, P. Nath, *Phys. Rev.* **D53** (1996) 1648;
T. Moroi, *Phys. Rev.* **D53** (1996) 6565;
M. Carena, G.F. Giudice, C.E.M. Wagner, *Phys. Lett.* **B390** (1997) 234;
M. Krawczyk, J. Zochowski, *Phys. Rev.* **D55** (1997) 6968.
- [6] N. Cabibbo, *Phys. Rev. Lett.* **10** (1963) 531;
M. Kobayashi, T. Maskawa, *Prog. Theor. Phys.* **49** (1973) 652.
- [7] For recent reviews on CP violation see e.g.:
K. Gronau, D. London, *Phys. Rev.* **D55** (1997) 2845;
Y. Grossman, Y. Nir, R. Rattazzi, hep-ph/9701231;
Y. Nir, hep-ph/9709301;
X.-G. He, hep-ph/9710551.

- [8] G.R. Farrar, M.E. Shaposhnikov, *Phys. Rev.* **D50** (1994) 774;
M.B. Gavela et al., *Nucl. Phys.* **B430** (1994) 382;
P. Huet, E. Sather, *Phys. Rev.* **D51** (1995) 379.
- [9] W. Buchmüller, D. Wyler, *Phys. Lett.* **B121** (1983) 321;
J. Polchinski, M.B. Wise, *Phys. Lett.* **B125** (1983) 393;
F. del Aguila, M.B. Gavela, J.A. Grifols, A. Méndez, *Phys. Lett.* **B126** (1983) 71 [E:
Phys. Lett. **B129** (1983) 473].
- [10] M. Dugan, B. Grinstein, L.J. Hall, *Nucl. Phys.* **B255** (1985) 413.
- [11] J.M. Frere, M.B. Gavela, *Phys. Lett.* **B132** (1983) 107.
- [12] S. Dimopoulos, S. Thomas, *Nucl. Phys.* **B465** (1996) 23.
- [13] N. Turok, J. Zadrozny, *Nucl. Phys.* **B369** (1992) 729;
M. Dine, P. Huet, R. Singleton Jr., *Nucl. Phys.* **B375** (1992) 625;
A. Cohen, A. Nelson, *Phys. Lett.* **B297** (1992) 111;
D. Comelli, M. Pietroni, A. Riotto, *Phys. Lett.* **B343** (1995) 343;
P. Huet, A.E. Nelson, *Phys. Rev.* **D53** (1996) 4578;
M. Aoki, N. Oshimo, A. Sugamoto, *Prog. Theor. Phys.* **98** (1997) 1179, *Prog. Theor. Phys.* **98** (1997) 1325, hep-ph/9706500;
M. Carena, M. Quirós, A. Riotto, I. Vilja, C.E.M. Wagner, *Nucl. Phys.* **B503** (1997) 387;
G.M. Cline, M. Joyce, K. Kaimulaine, *Phys. Lett.* **B417** (1998) 417.
- [14] X.-G. He, B.H.J. Mc Kellar, S. Pakvasa, *Int. Jour. Mod. Phys.* **A4** (1989) 5011;
W. Bernreuther, M. Suzuki, *Rev. Mod. Phys.* **63** (1991) 313;
Y. Kizukuri, N. Oshimo, *Phys. Rev.* **D45** (1992) 1806, *Phys. Rev.* **D46** (1992) 3025;
S. Bertolini, F. Vissani, *Phys. Lett.* **B324** (1994) 164.
- [15] J.F. Donoghue, *Phys. Rev.* **D18** (1978) 1632;
E.P. Shabalin, *Sov. J. Nucl. Phys.* **28** (1978) 75;
A. Czarnecki, B. Krause, *Phys. Rev. Lett.* **78** (1997) 4339.
- [16] N.F. Ramsey, *Annu. Rev. Nucl. Part. Sci.* **40** (1990) 1;
I.S. Altarev et al., *Phys. Lett.* **B276** (1992) 242.
- [17] J. Bailey et al., *J. Phys.* **C4** (1978) 345, *Nucl. Phys.* **B150** (1979) 1;
Y. Semertzidis et al., E821 Collaboration at BNL, *AGS Expression of Interest: Search for an Electric Dipole Moment of Muon*, September 1996.
- [18] P. Nath, *Phys. Rev. Lett.* **66** (1991) 2565.

- [19] R. Kuchimanchi, *Phys. Rev. Lett.* **76** (1996) 3486;
R. Mohapatra, A. Rasin, *Phys. Rev. Lett.* **76** (1996) 3490;
Y. Nir, A. Rattazzi, *Phys. Lett.* **B382** (1996) 363.
- [20] E. Christova, M. Fabbrichesi, *Phys. Lett.* **B315** (1993) 113, *Phys. Lett.* **B315** (1993) 338, *Phys. Lett.* **B320** (1994) 299;
B. Grzadkowski, W.Y. Keung, *Phys. Lett.* **B316** (1993) 137;
M. Aoki, N. Oshimo, hep-ph/9808217.
- [21] ECFA/DESY LC Physics Working Group, *Phys. Rep.* **299** (1998) 1.
- [22] R. Garisto, J.D. Wells, *Phys. Rev.* **D55** (1997) 1611.
- [23] T. Ibrahim, P. Nath, *Phys. Lett.* **B418** (1998) 98, *Phys. Rev.* **D57** (1998) 478 [E: *Phys. Rev.* **D58** (1998) 019901], hep-ph/9807501.
- [24] T. Falk, K.A. Olive, *Phys. Lett.* **B439** (1998) 71.
- [25] M. Brhlik, G.J. Good, G.L. Kane, hep-ph/9810457.
- [26] S.A. Abel, *Phys. Lett.* **B410** (1997) 173.
- [27] F. Gabbiani, A. Masiero, *Nucl. Phys.* **B322** (1989) 235;
G.S. Hagelin, S. Kelley, T. Tanaka, *Nucl. Phys.* **B415** (1994) 293;
F. Gabbiani, E. Gabrielli, A. Masiero, L. Silvestrini, *Nucl. Phys.* **B477** (1996) 321.
- [28] J. Bernabéu, G.A. González-Sprinberg, M. Tung, J. Vidal, *Nucl. Phys.* **B436** (1995) 474.
- [29] J. Bernabéu, G.A. González-Sprinberg, J. Vidal, *Phys. Lett.* **B397** (1997) 255.
- [30] J. Bernabéu, G.A. González-Sprinberg, J. Vidal, *Phys. Lett.* **B326** (1994) 168.
- [31] J. Bernabéu, G.A. González-Sprinberg, J. Vidal, in *Proceedings of the Ringberg Workshop on Perspectives for electroweak interactions in e^+e^- collisions*, ed. B.A. Kniehl, World Scientific 1995, p. 329.
- [32] B. Mele, G. Altarelli, *Phys. Lett.* **B299** (1993) 345;
B. Mele, *Mod. Phys. Lett.* **A49** (1994) 1239.
- [33] J. Bernabéu, D. Comelli, L. Lavoura, J. P. Silva, *Phys. Rev.* **D53** (1996) 5222.
- [34] W. Hollik, J.I. Illana, S. Rigolin, D. Stöckinger, *Phys. Lett.* **B416** (1998) 345;
B. de Carlos, J.M. Moreno, *Nucl. Phys.* **B519** (1998) 101.
- [35] G.C. Branco, M.N. Rebelo, *Phys. Lett.* **B160** (1985) 11;
S. Weinberg, *Phys. Rev.* **D42** (1990) 860;
W. Bernreuther, T. Schröder, T.N. Pham, *Phys. Lett.* **B279** (1992) 389.

- [36] W. Bernreuther, A. Brandenburg, P. Overmann, *Phys. Lett.* **B391** (1997) 413.
- [37] W. Hollik, J.I. Illana, S. Rigolin, D. Stöckinger, *Phys. Lett.* **B425** (1998) 322.
- [38] A. Bartl, E. Christova, W. Majerotto, *Nucl. Phys.* **B460** (1996) 235 [E: *Nucl. Phys.* **B465** (1996) 365];
A. Bartl, E. Christova, T. Gajdosik, W. Majerotto, *Nucl. Phys.* **B507** (1997) 35 [E: *Nucl. Phys.* **B531** (1998) 653].
- [39] C. Itzykson, J. Zuber, *Quantum Field Theory*, McGraw–Hill, 1985, p. 160.
- [40] S. Ferrara, E. Remiddi, *Phys. Lett.* **B53** (1974) 347;
I. Giannakis, J.T. Liu, M. Porrati, *Phys. Rev.* **D58** (1998) 045016.
- [41] J.M. Cornwall, *Phys. Rev.* **D26** (1982) 1453.
- [42] J. Papavassiliou, C. Parrinello, *Phys. Rev.* **D50** (1994) 3059.
- [43] A. Denner, S. Dittmaier, G. Weiglein, *Phys. Lett.* **B333** (1994) 420, *Nucl. Phys.* **B440** (1995) 95.
- [44] T. Appelquist, J. Carrazzone, *Phys. Rev.* **D11** (1975) 2856;
A. Dobado, M.J. Herrero, S. Peñaranda, hep-ph/9710313, hep-ph/9806488.
- [45] W. Bernreuther, G.W. Botz, O. Nachtmann, P. Overmann, *Z. Phys.* **C52** (1991) 567;
W. Bernreuther, O. Nachtmann, P. Overmann, T. Schröder, *Nucl. Phys.* **B388** (1992) 53 [E: *Nucl. Phys.* **B406** (1993) 516].
- [46] W. Hollik, C. Schappacher, hep-ph/9807427.
- [47] H.-Y Zhou, *Phys. Rev.* **D58** (1998) 114002, hep-ph/9806323.
- [48] W. Bernreuther, P. Overmann, *Z. Phys.* **C72** (1996) 461.
- [49] W. Bernreuther, O. Nachtmann, *Phys. Rev. Lett.* **63** (1989) 2787 [E: *Phys. Rev. Lett.* **64** (1990) 1072];
W. Bernreuther, O. Nachtmann, P. Overmann, *Phys. Rev.* **D48** (1993) 78.
- [50] A. Brandenburg, M. Flesch, P. Uwer, hep-ph/9806306;
J. Kodaira, T. Nasuno, S. Parke, hep-ph/9807209.
- [51] A. Czarnecki, M. Jezabek, J.H. Kühn, *Nucl. Phys.* **B351** (1991) 70.
- [52] D. Atwood, A. Soni, *Phys. Rev.* **D45** (1992) 2405;
M. Diehl, O. Nachtmann, *Z. Phys.* **C62** (1994) 397.

- [53] C.R. Schmidt, M.E. Peskin, *Phys. Rev. Lett.* **69** (1992) 410;
 C.R. Schmidt, *Phys. Lett.* **B293** (1992) 111;
 D. Chang, W.-Y. Keung, I. Phillips, *Nucl. Phys.* **B408** (1993) 286 [E: *Nucl. Phys.* **B429** (1994) 255].
- [54] W. Bernreuther, U. Löw, J.P. Ma, O. Nachtmann, *Z. Phys.* **C43** (1989) 117.
- [55] A. Bartl, E. Christova, T. Gajdosik, W. Majerotto, hep-ph/9712380.
- [56] S. Bar-Shalom, D. Atwood, A. Soni, *Phys. Rev.* **D57** (1998) 1495;
 M. Aoki, N. Oshimo, hep-ph/9801294.
- [57] W. Beenakker, S.C. van der Marck, W. Hollik, *Nucl. Phys.* **B365** (1991) 24.
- [58] A. Denner, *Fortschr. Phys.* **41** (1993) 307.
- [59] H.E. Haber, G.L. Kane, *Phys. Rep.* **117** (1985) 75;
 J.F. Gunion, H.E. Haber, *Nucl. Phys.* **B272** (1986) 1 [E: *Nucl. Phys.* **B402** (1993) 567];
 J.F. Gunion, H.E. Haber, G.L. Kane, S. Dawson, *The Higgs Hunter's Guide*, Addison-Wesley 1990.
- [60] H.E. Haber, in *Proc. of the 1992 Theoretical Advanced Study Institute in Particle Physics*, ed. J. Harvey and J. Polchinski (World Scientific, Singapore, 1993), p. 583.